


# An Insight of Nanomaterials in Tissue Engineering from Fabrication to Applications

Ritika Sharma<sup>1</sup> · Sanjeev Kumar<sup>2,3</sup> · Bhawna<sup>2,3</sup> · Akanksha Gupta<sup>4</sup> · Neelu Dheer<sup>5</sup> · Pallavi Jain<sup>6</sup> · Prashant Singh<sup>7</sup>  · Vinod Kumar<sup>2,8</sup>

Received: 20 November 2021 / Revised: 17 March 2022 / Accepted: 8 April 2022 / Published online: 4 June 2022  
© Korean Tissue Engineering and Regenerative Medicine Society 2022

Tissue engineering is a research domain that deals with the growth of various kinds of tissues with the help of synthetic composites. With the culmination of nanotechnology and bioengineering, tissue engineering has emerged as an exciting domain. Recent literature describes its various applications in biomedical and biological sciences, such as facilitating the growth of tissue and organs, gene delivery, biosensor-based detection, etc. It deals with the development of biomimetics to repair, restore, maintain and amplify or strengthen several biological functions at the level of tissue and organs. Herein, the synthesis of nanocomposites based on polymers, along with their classification as conductive hydrogels and bioscaffolds, is comprehensively discussed. Furthermore, their implementation in numerous tissue engineering and regenerative medicine applications is also described. The limitations of tissue engineering are also discussed here. The present review highlights and summarizes the latest progress in the tissue engineering domain directed at functionalized nanomaterials.

**Keywords** Tissue engineering · Nanomaterials · Nanotechnology · Regenerative medicine · Biomimetics · Conductive hydrogels · Polymers · Scaffolds

## 1 Introduction

In tissue engineering (TE) domain, tissue growth is initiated by 3D-scaffolds; the cells proliferate and differentiate into several types or from a base of cells. These scaffolds are combined with growth factors (GFs) to direct cell behaviour and enable the production of tissue. These

engineered tissues are functional and capable of implant growth and regeneration [1–5]. Currently, it has become an impressive tool for repairing and reconstructing impaired organs and tissues. In the past two decades, the immense implementation of nanomaterials (NMs) in TE has progressed tremendously (Fig. 1).

---

✉ Akanksha Gupta  
akankshachem05@gmail.com

✉ Prashant Singh  
psingh@arsd.du.ac.in

✉ Vinod Kumar  
kumarv@mail.jnu.ac.in

<sup>1</sup> Department of Biochemistry, University of Delhi, Delhi, India

<sup>2</sup> Department of Chemistry, Kirori Mal College, University of Delhi, Delhi, India

<sup>3</sup> Department of Chemistry, University of Delhi, Delhi, India

<sup>4</sup> Department of Chemistry, Sri Venkateswara College, University of Delhi, Delhi, India

<sup>5</sup> Department of Chemistry, Acharya Narendra Dev College, University of Delhi, Delhi, India

<sup>6</sup> Department of Chemistry, SRM Institute of Science and Technology, Delhi NCR Campus, Ghaziabad, Uttar Pradesh, India

<sup>7</sup> Department of Chemistry, Atma Ram Sanatan Dharma College, University of Delhi, Delhi, India

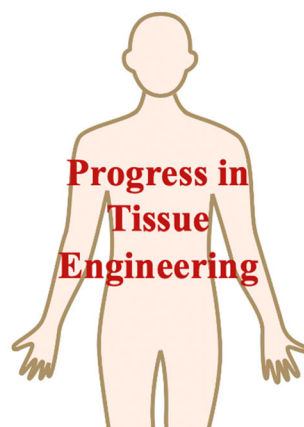
<sup>8</sup> Special Centre for Nano Science, Jawaharlal Nehru University, Delhi, India

Various cell sources, such as iPSCs and adult stem cells, have become available, as have genetic editing tools that allow for more cell customization. Chemical advances and GF delivery systems, biophysical signals on cellular functions and tissue design strategies have contributed to building tissues that are architecturally, compositionally and functionally identical to their natural counterparts [6]. The advent of nanoparticles (NPs) is linked to their nanoscale dimensions, which allow them to diffuse through the membrane and aid in cellular uptake.

Several NMs have been developed for their unique and exceptional physicochemical characteristics and biocompatibility, making them a potential candidate for modelling tissue-engineered bioscaffolds. These scaffolds play a prominent role in controlling and regenerating tissues to provide structural support. These have been utilized in numerous processes, such as bone repair, neural regeneration, wound healing, etc. [4]. In the past decade, extraordinary advancements have been made in implementing nanotechnology in neuroscience and neuro-engineering. It is prescient that such novel nanotechnologies would bring crucial insights into bioengineering [7].

NMs possess excellent biocompatibility, inherent optical properties, surface functionality, large surface area, biodegradability, etc. and thus can be utilized *in vivo* and *in vitro* research for tissue and organ construction [4, 8–10]. Two-dimensional (2D) NMs are a category of materials possessing one-dimension atomic layer thickness and exhibit excellent properties because of their unique nano-plane. The most commonly used 2D NM is graphene [4, 11–13]. Furthermore, 3D bioscaffolds have a systematized framework, are inspired by biomimetics and have grabbed immense attention [14, 15].

**Fig. 1** Summary of tissue engineering progress in the past decade [6] (Reconstructed from [Khademhosseini A, Langer RA. decade of progress in tissue engineering. Nat Protoc. 2016;11:1775–81])

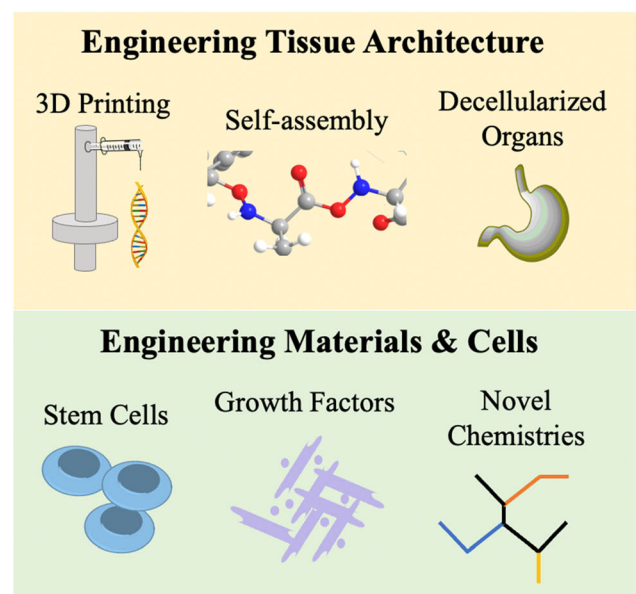


This review highlights the fabrication process of bioscaffolds and conductive hydrogels using functionalized NMs and their applications in bioengineering and regeneration. In many instances, conductive hydrogels and bioscaffolds are used interchangeably. However, they possess different characteristics. Indeed, conductive hydrogels have the edge over bioscaffolds for TE innovation. Herein, we have discussed and summarized NMs used in various cardiac, nerve, bone, dental and skin TE applications developed so far.

## 2 Operational definition, types, advantages and disadvantages

TE is an interdisciplinary area that amalgamates material science, biological science, and engineering. It is concerned with the development of biomimetics to repair, restore, maintain and amplify or strengthen a variety of biological functions at the tissue and organ levels [1–4]. NPs have tremendously contributed to this field. However, they are not confined to fixed sizes; they can be customized or fabricated in various sizes and shapes that lead to purpose-oriented characteristics and mimic several components of the extracellular matrix (ECM). It plays an indispensable role in establishing an organ's structural framework [4].

Nanocomposites are comprised of two or more materials that mainly include NMs and polymers. Polymeric NPs can be classified as (1) natural and (2) synthetic and are widely used. Both types of polymers have several advantages and limitations, such as the natural polymer's cell adhesion support. In contrast, synthetic polymers are better



controllable, inert and tunable, but they do not mimic the ECM [16]. Natural polymers are inseparable from TE, despite having several limitations, such as processability, mechanical, electrical and physicochemical properties and variations that could cause an immune response [16–18]. Recently, biodegradable polymeric NPs have gained recent consideration due to numerous characteristics such as structural precision, porosity, degradation, etc. Commonly used biodegradable polymers are poly(lactic acid), polycaprolactone (PCL), poly(p-dioxanone), poly(glycolic acid), etc., which are either naturally or synthetically derived [19]. Therefore, modulating polymers with NPs could improve properties and compatibility, thereby minimizing their limitations.

Polymers functionalized with NMs, biomolecules or stem cells can be categorized based on their ability to mimic the ECM into (1) bioscaffolds and (2) conductive hydrogels. The literature reveals that conductive hydrogels mimic the ECM more efficiently as compared to scaffolds. Conductive hydrogels with enhanced strength and conductivity have been developed using poly(ethylene glycol) (PEG), poly(vinyl alcohol) (PVA), and graphene oxide (GO) NPs [20, 21]. They are constructed using a blending method that could lead to agglomeration of conductive material formed in hydrogel and this drawback leads to an in situ process that provides a high level of flexibility and strength [20, 22].

Hydrogels turned out to be employed in the TE domain to stimulate the functions of native tissues, as they can form a 3D polymeric network possessing several shapes and sizes due to unique physical properties [20, 23]. To replicate the biological and electrical characteristics, one of the most efficient materials is a conductive hydrogel, which is an amalgamation of conductive polymers and soft hydrogels [20, 24, 25]. Due to their unique characteristics, conductive hydrogels efficiently provide electrical conductivity to cells [20]. It also improves cell adhesion, differentiation, proliferation, and migration and has a huge role in bioengineering of various tissue types [26].

Of several types of NMs, metal and carbon-based NMs have been used in several applications because of their electrical properties and have restricted use due to cytotoxicity and homogenous distribution [20, 26]. Magnetic NPs have emerged to have crucial roles in applications associated with the biomedical sector. The use of magnetic NPs for cell growth and seeding makes them suitable for a practical regenerative medicine approach [27]. Different functionalized NMs used do not just act as a supporting material but are crucial for enhancing the efficacy of various TE applications and regenerative medicine. They exhibit excellent mechanical and electrical properties and improve mechanical strength, cause uniform distribution, and reduce electrical impedance to the scaffold.

Furthermore, they have antimicrobial properties, good biocompatibility, reduced cytotoxicity, etc. This adds to its immense utilization [20]. Therefore, the following section has briefly highlighted the functionalization of NMs and polymer materials.

### 3 Functionalization of nanomaterials

Functionalization and modification of NMs onto the surface of biomaterials or stem cells are of utmost importance, as this mainly accounts for cell function, regulation and NM implantation. Functionalized NMs are those materials whose characteristics and properties are enhanced by their surface modification. NMs have the appropriate size, composition, structure, and surface chemistry. Therefore, the combination of polymeric NPs could improve surface area, biocompatibility and many more such characteristics. Hence, proper functionalization could revolutionize TE research. Doberenz et al. investigated thermo-responsive polymers for biomedical applications. These can be triggered by several stimuli, such as pH, temperature, light, enzymes, ionic strength, and others, leading to modulation of physical characteristics. It enables the implant or material property to be influenced by environmental conditions. Hence, they are gaining an interest in the biomedical field [28].

Another example is nanofibrillated cellulose (NFC), which is a plant-derived polysaccharide that possesses large surface area, size (5–20 nm), flexibility, and good mechanical strength and thus is utilized for the fabrication of strong and lightweight scaffolds [29, 30]. In addition, these are known to biomimetic collagen's mechanical functions [31]. NFC can be derived from cotton, rice, bananas, wood pulp, corn, palm, soya beans, etc. via ultracentrifugation, ultrasonication, acid hydrolysis, and bleaching processes, etc. Nasri-Nasrabadi et al. used a chemo-mechanical method to extract NFC from rice with a length of 4–5 cm, which was then modified by starch via a coalescence of film casting, salt leaching and freeze-drying process for engineering cartilage. Cellulose and starch are connected by a rigid hydrogen network that generates the transfer of stress from matrix to nanofibers. The scaffold is attached to the chondrocyte cells via the formation of filopodia and the cells cover the entire scaffold in 7 days by incorporating nanocellulose into the starch matrix. Therefore, cell attachment and proliferation are improved [32].

Zhang et al. modified bacterial cellulose nanofiber (BCN) with lecithin as *Acetobacter xylinum* X-2 bacteria using immersion and subsequent proanthocyanidin (PA) cross-linking. *Acetobacter xylinum* X-2 bacteria are cultured in media containing 5 wt% sucrose and 0.3 wt% green tea powder for a week at pH 4.5. BCN is rinsed in an

alcohol solution containing different concentrations of lecithin (1–2 wt%) with stirring with the help of an orbital shaking incubator for a day. After that, the cross-linking process is initiated by rinsing the synthesized sample in a 0.05 wt% PA solution. PA cross-linking can stop the detachment of lecithin from BCN. Pristine BC has a semi-transparent white color that turns yellow with increasing lecithin concentration in alcohol and 2 wt% lecithin layers completely wrapped around BCN by weak physical adsorption. Lecithin causes a decrease in hydrophilicity, storage modulus, and thermal stability until BC/LECs are preferable over other natural polymer scaffolds. MDA-MB-231 cells are well-spread and adhered to the scaffold after 7 days, suggesting favorable cell proliferation [33]. A promising alternative for NFC is carboxymethyl cellulose (CMC), a structural analogue that has a chemical resemblance to NFC through interfacial adhesion and thus could add strength, robustness and flexibility to the printed tissue scaffold [14, 34]. Multi-step chemical cross-linking methods have been demonstrated to improve the mechanical strength and stability of bioscaffolds [35].

For human tissue differentiation and regeneration, several scaffolds have emerged with the potential to mimic ECM [14, 15]. For the synthesis and functionalization of NMs, scaffolds and hydrogels, a range of techniques are available that involve: (1) the electrospinning method, (2) 3D/4D printing, (3) direct ink writing (DIW), (4) freeze-drying, (5) injection molding, (6) spray pyrolysis, (7) blending, (8) in situ, (9) coating, (10) co-precipitation, etc. [14, 36]. A major challenge associated with these techniques is the fabrication of scaffolds with optimized porosity, morphology, and interconnectivity. However, 3D printing is starting to overcome this limitation by fabricating customized scaffolds with high design flexibility and structural complexity for soft tissue such as cartilage and hard tissue such as bone [15, 37, 38]. Due to its effectiveness in scaffold fabrication, 3D printing and DIW have received much interest [14, 15]. Various nanomaterials and nanostructured scaffolds are classified based on the aforementioned synthesis methods as in Table 1. A few of the previously mentioned functionalization methods are highlighted in the following subsection.

### 3.1 Direct ink writing method

Hydrogels are ejected via an outlet to construct scaffolds having complex and exquisite features. Scaffolds require spatial resolution and a meshwork of macropores (200–400  $\mu\text{m}$ ) and micropores (40–100  $\mu\text{m}$ ) to facilitate tissue ingrowth and cell adhesion, respectively [38, 87]. However, the amalgamation of macropores and micropores is challenging and cannot be achieved by DIW alone. Therefore, to circumvent this shortcoming, 3D printing is

employed for the initiation of spatially resolved macropores and using the freeze-drying method [88] for networked micropores [14, 89, 90]. Such scaffolds can be fabricated with several biomaterials, but cytocompatibility, availability, solubility in aqueous solutions and dispersibility have led to increased utilization of polysaccharides as synthetic biomaterials [91].

### 3.2 Electrospinning method

It is a hydrodynamic process that involves four consecutive steps: (1) electrification of the liquid jet and the formation of a Taylor cone, (2) whipping motions, (3) electric bending instability, and (4) solidification of the jet to obtain a solid fibre (Fig. 2). In this process, fibres are generated by the stretching and elongation of a jet, produced by the electrification of a liquid drop. Electrification is followed by Taylor cone formation through the deformation of the droplet of the same sign as a consequence of electrostatic repulsion between surface charges. The jet undergoes whipping motions after extending into a straight line. The solid fibres get deposited onto the grounded collector when stretched into finer diameters [92].

Modified cellulose (MC) is fabricated with PVA nanofiber via an electrospinning method for bone TE by Chahal et al. Startingly, the blend solutions of different wt% PVA/MC are synthesized using water as the solvent to functionalize nanofibers. For electrospun, the PVA/MC polymer solution is filled into a plastic syringe with a hypodermic needle. This needle is connected to the high voltage power supply's positive electrode with the help of copper wires, while the negative electrode is connected to a foil of aluminium that works as a collector. The electrospun nanofibers are collected through the aluminium foil collector. The nanofibers' crystallinity decreases with a decrease in PVA percentage for the blend's solution. The nanofibers' low crystallinity is preferable for bone TE as it improves the scaffold mechanical properties [43].

### 3.3 Spray pyrolysis method

This method involves the use of metal–organic precursors in organic solvents to obtain a homogenous, non-cracked deposition (Fig. 3). The deposition parameters are: nozzle distance to substrate, deposition temperature, flow rate of solution, concentration of precursor and carrier gas flow rate. In the procedure, the precursor solution is atomized into droplets. These droplets are then carried by carrier gas into a thermolysis chamber and then to the calcination furnace. The droplets are dried after being evaporated and precipitated. Thermolysis reactors decompose the dried particles into microporous particles that are sintered into

**Table 1** Classification of NMs and nanostructured scaffolds based on their fabrication methods

Synthesis method	NMs/nanostructured scaffolds	References
Freeze-drying method	NFC	[29, 30, 39, 40]
Cross-linking method	CS/GO-Au scaffolds	[20, 33, 35, 41, 42]
	CNT/PVA	
Electrospinning method	BCN	[43–50]
	CMC	
	Au/photo-curable gelatin hydrogel	
	MC/PVA	
	MoS <sub>2</sub> /rGO/SF nanofibers	
	PPy/SF nanofibers	
	Poly(L, D-lactide) fibers/collagen I hydrogel	
Polymerization method	GO/CS/PVP	[20, 51–57]
	GO/CS/HA containing osteogenesis inducing drug SV	
	CNT/PBAT fibers	
	GO-PLGA/Col hybrid fiber sheets	
	CNT/polyaniline	
	PEDOT/PSS	
	Au NP/1,3,5-benzene tricarboxylic acid/Fe <sup>3+</sup> ion	
	Flu-loaded nanoporous PPy	
	Cellulose/pyrrole monomer	
	CSH/PAA/Dch-PPy	
CVD method	CS-Gel/nZnO scaffolds	[58–60]
	MoSe <sub>2</sub> -NIPAM hydrogels	
	Pristine MWCNT/PPy	
EDC/NHS method	CNT/HA	[4, 61–63]
	3D GF	
	HA-DA/rGO hydrogels	
	fGO/DNA <sub>VEGF</sub> /GelMA	
Robocasting method	HA-DA/rGO hydrogel dressing	[64]
	GO-PEG/Que/Col scaffold	
Improved Hummer's method	PCL scaffolds/GNPs	[64]
Hydrolysis method	GO/CS/DA	[20, 65]
Electrospraying method	TiO <sub>2</sub> /PEGylated CS	[20, 66]
	GO/alginate microgels	[67]
IBAD/IME method	rGO/alginate microgels	[68–75]
	TiN microelectrode arrays	
Ionic modification and ultrasonic treatment	MWCNTs/PCL scaffold	[76, 77]
Covalent attachment	Mesoporous silica/PAMAM	[76]
Coating method	Au/immobilized silica spheres	[4, 9, 76, 78, 79]
	BP nanosheets/GelMA nanocomposite	
	BP/natural polymers	
Centrifugal spinning/micro-cutting method	GO-BP scaffold	[80]
Sonication and thermal curbing	M.SF/alginate hydrogels	[80]
In situ crystallization	PEG-GO/PPF	[4, 81]
	GO/CS/nHAP	[4, 82]
Dry mechanochemical method	GO/PMMA/PLC/FA	[83]
Pulverization method	GO/PMMA/PLC/FA	[83]
Photo-immobilization method	CNT/3D Collagen scaffold/β-tricalcium phosphate	[84]
Facile mixing method	CNT/surface-modified PCL/PLA scaffold/insulin-like GF I	[85]
	CS-g-PA/PEG-co-PGS	[20, 86]

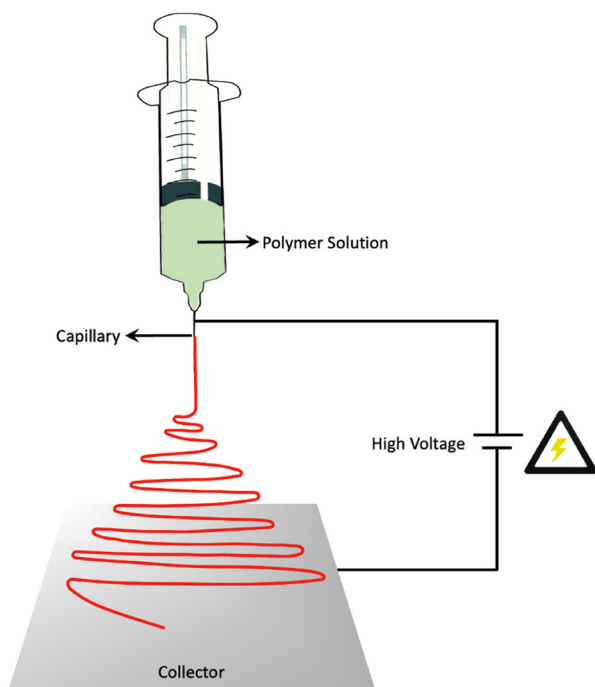


**Fig. 2** Schematic illustration of the synthesis of the NM-based polymer composites via electrospinning method

the calcination furnace. This method produces high-purity NPs with homogenous chemical compositions [93].

### 3.4 Injection modelling method

This method is known to include three stages: (1) filling, (2) injection and (3) holding. First of all, the screw moves the material in a forward direction at a certain speed. With the shallowing of the screw groove, the compact material is conveyed forward. During the injection process, the injection machine fills the material into the mold with an increase in back pressure. To ensure the safe molding of the injected material, the temperature is decreased in order to reduce pressure in the mold cavity. Finally, the injection mold is opened to eject the material without being damaged [94].

### 3.5 Freeze drying method

A polymeric solution of the desired polymer is prepared in a solvent and kept for polymerization (Fig. 4). To separate the solvent from the solution, the temperature and pressure are kept low. The solvent is sublimed to give a solid scaffold structure. By varying the pH and freezing rate, the porosity of the structure is monitored. Time consumption and relatively smaller pore sizes are added limitations to this method [95].

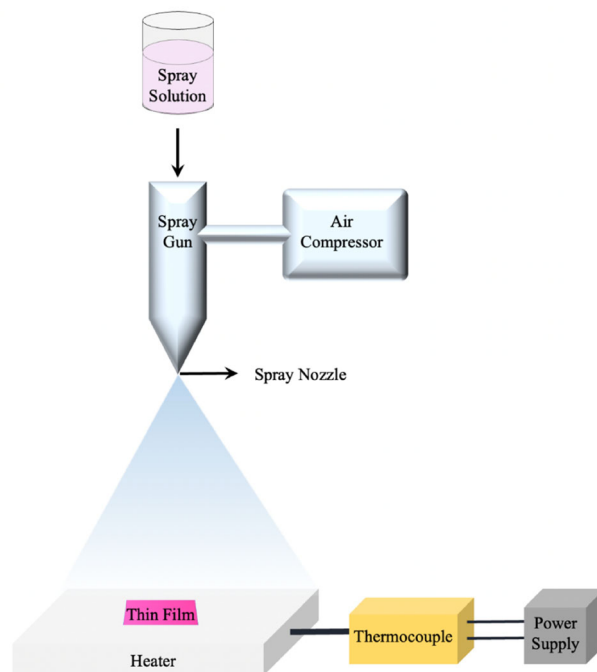


**Fig. 3** Schematic illustration of the synthesis of the NM-based polymer composites via spray pyrolysis method

### 3.6 3D/4D printing

Several research areas utilize next-generation fabrication strategies like 3D and 4D printing. 3D printing permits the synthesis of highly precise and complex materials. It is a manufacturing technique in which different layers are overlapped over one another to form 3D components. Figure 5 demonstrates the biofabrication of bioinks using cells, bioactive fillers, and polymers. The composite bioink is then passed through the dispenser, resulting in the layer-by-layer construction of the desired polymer composite [96]. Whereas, 4D printing takes 3D printing as a starting point and adds a new dimension of revolution. It enables excellent materials to modulate their properties, such as shape or color, to become bioactive by forming dynamic 3D structures and to perform desired functions in response to external stimuli or environmental factors such as temperature, humidity and light [97]. Therefore, they have been widely explored for the invention of bioscaffolds [98, 99].

### 3.7 In situ polymerization method

For the synthesis of conductive hydrogels, the introduction of a conductive component into a non-conductive hydrogel by polymerization can be achieved using an in situ growth mechanism. In situ preparation of polymer composites and CNTs distributed throughout the hydrogel enabled them to

**Fig. 4** Schematic illustration of the synthesis of NM-based polymer composites via spray pyrolysis method

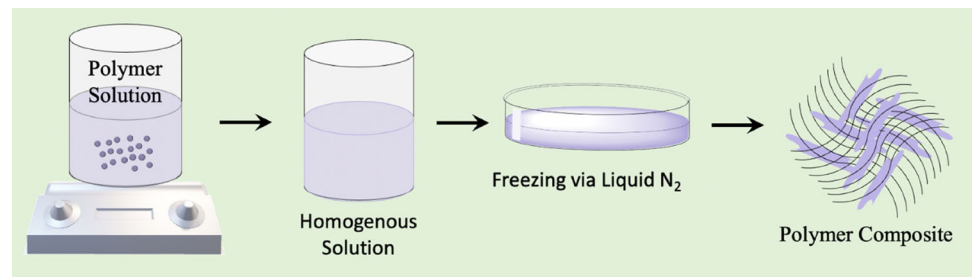
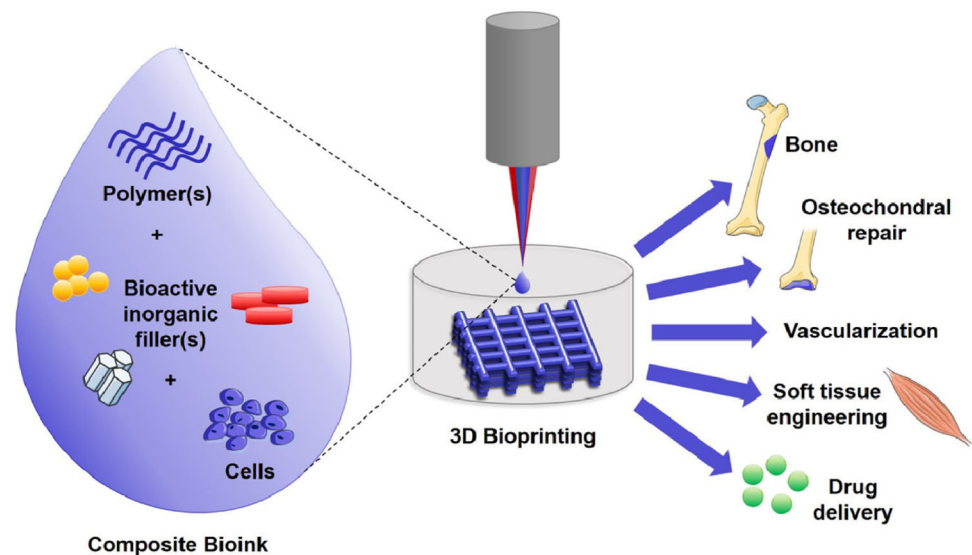


**Fig. 5** Schematic illustration of 3D bioprinting for personalized implants and tissue scaffolds. Reprinted with permission, [96] Copyrights © 2020 The Authors. Published by Elsevier Ltd on behalf of Acta Materialia Inc



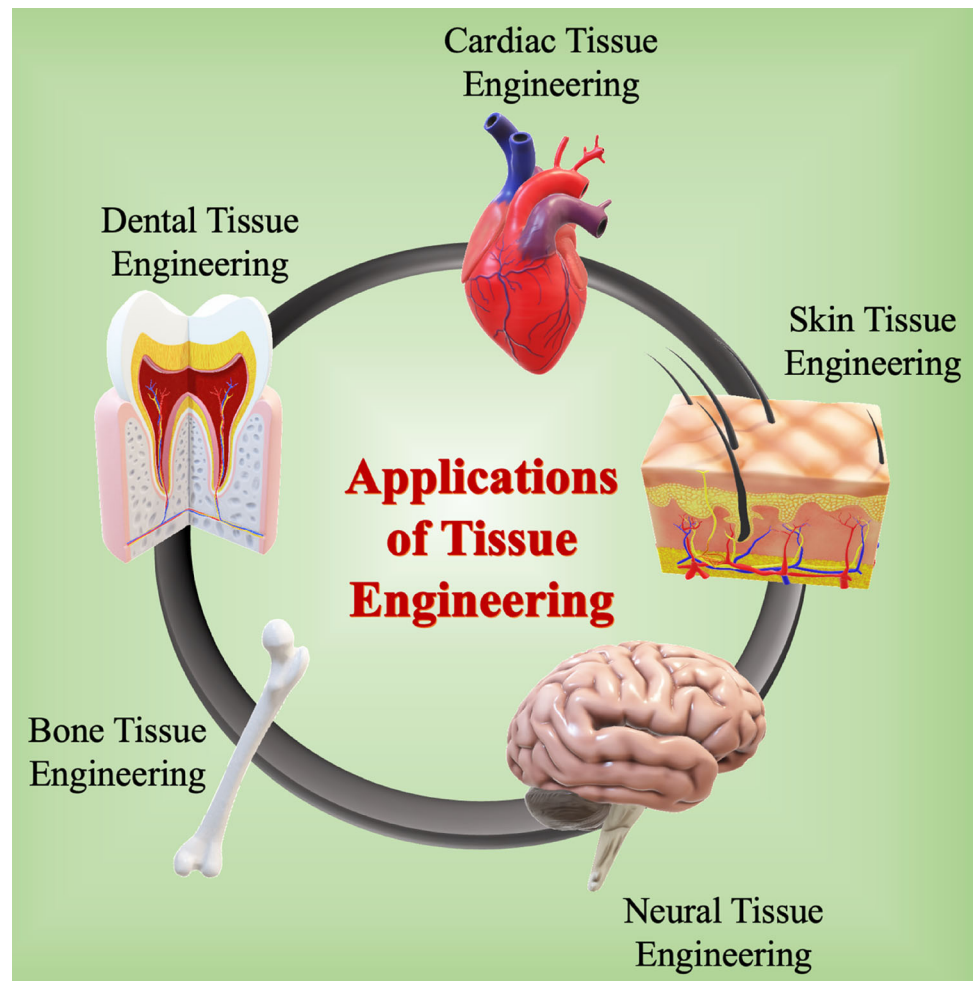
possess homogenous conductivity, better reliability, and amplifies the strength of conductive hydrogels. Yang et al. used a plasma technique and in situ polymerization to functionalize conductive CNTs with polyaniline. CNTs are dissolved in deionized water by sonication. After that, aniline and HCl solution are added under continuous stirring followed by dropwise addition of an aqueous solution of ammonium peroxydisulfate. The reaction is monitored for about 2 h or till the deep green product is obtained [51]. Kim et al. prepared a PEG-based hydrogel using sequential two-step polymerization by in situ polymerization of poly(3,4-ethylenedioxythiophene) (PEDOT) within poly(4-styrenesulfonic acid) (PSS) for the generation of a cardiac scaffold. The solution of the hydrogel precursor is prepared by dissolving 50% w/w PEG-diacrylate in water. The prepared solution is mixed with 5% v/v 2-hydroxy-2-methylpropiophenone and 25% v/v PSS, followed by pouring onto a silica mold. Further, the above solution is dipped in 3,4-ethylenedioxythiophene (EDOT) monomer under UV irradiation. The polymerization of EDOT is initiated after the completion of EDOT loading in the hydrogel. This can be done by dissolving it in an ethanol solution containing 5% v/v H<sub>2</sub>SO<sub>4</sub> and Fe-tosylate at room temperature and finally getting a highly conductive

hydrogel. A small amount of sulfuric acid was added to the hydrogel to enhance polymerization and conductivity. The conductive hydrogel is non-adhesive towards myocyte H9C2 cells and proteins, and therefore, RGD peptides were attached covalently via a 5-azidonitrobenzoyloxy-NHS linker that was fixed photochemically to the hydrogel surface [52].

### 3.8 Chemical vapor deposition method

For the development of conductive hydrogels, techniques such as the growth of metal NPs in bulk hydrogels [14, 100], polymerization of conductive polymers [20, 101], and CNT deposition via chemical vapor deposition (CVD) [20] have been used. Pristine MWCNTs have been synthesized in homemade CVD using acetylene gas at a temperature of 700 °C and further coated with PPy monomers via in situ chemical polymerization by Gupta et al. The polymerization of PPy is done by drop casting of a mixture of ammonium persulphate (0.1 M) and 35% HCl. The amorphous nature of PPy remains constant after coating onto MWCNTs. The composite of PPy and MWCNTs forms a core shell structure, with MWCNT and

**Fig. 6** Schematic representation of various applications of tissue engineering such as bone-, nerve-, cardiac-, and skin-associated tissues



PPy forming the inner core and outer shell, respectively [58].

### 3.9 Other methods

Coating the surface of a hydrogel could easily provide conductivity with suitable physico-mechanical properties. The surface coating can be achieved by several methods, like reversible split chain transfer, spinner vision, and click chemistry onto the hydrogel surface [20]. An electrodeposited Au NPs conductive hydrogel was created by cross-linking 1,3,5-benzene tricarboxylic acid (ligand) and an  $\text{Fe}^{3+}$  ion [20, 41]. Conductive coating has several advantages in drug delivery and bioactive agents. There are certain limitations associated with it, such as peeling off due to low elasticity and differences in mechanical strengths, as the hydrogel and coating material act independently [20, 102]. Luo et al. developed a sponge-like conductive polymer (CP) PPy film. Fluorescein (Flu)-loaded nanoporous PPy film is made up of template-derived PPy on a fine protective layer. The nanoporous film is made more hydrophilic by immersing the modified PPy electrode

in water and ethanol. Subsequently, 0.5  $\mu\text{L}$  of Flu (0.01 M) is added dropwise onto the surface of the electrode to dry it naturally in the air. Flu is able to permeate the hydrophilic PPy films. A thin PPy film is electropolymerized on the top surface of a hydrophilic PPy film to prevent the leakage of stored drugs [53].

HA-DA/rGO hydrogels are formed by Liang et al. for wound dressing. Dopamine (DA) was linked to hyaluronic acid (HA) by the standard 1-(3-dimethylaminopropyl)-3-ethylcarbodiimide hydrochloride (EDC)/N-hydroxysuccinimide (NHS) method. Then, they were crosslinked with rGO@PDA by oxidative coupling between them through  $\text{H}_2\text{O}_2$ /horseradish peroxidase (HRP), resulting in hydrogel formation. Self-healing capability can thus arrest leakage of fluid along with bacterial penetration and infection after adhering to the wound site due to hydrogel deformation or fracture [61]. Deliormanlı investigated PCL scaffolds having a grid-like arrangement and periodic lattice that were synthesized via the robocasting method using graphene nanoplatelets (GNPs) for cartilage TE. The PCL was dissolved in anhydrous acetone to make a 20 wt% PCL solution. The different concentrations of GNPs were



**Table 2** Cardiac tissue engineering applications

Nanocomposite	Synthesis method	Highlights	References
fGO/DNA <sub>VEGF</sub> /GelMA	EDC/NHS coupling	Cardiac repair and vasculogenesis	[4, 62]
GO/CS/DA	Improved Hummer's method	Enhance viability and proliferation of myocardial stem cells Possess self-healing properties	[20, 65]
TiO <sub>2</sub> /PEGylated CS	Hydrolysis method and mixed with a matrix	Enhance cell retention and adhesion of myocardial cells Show excellent cell-hydrogel matrix interactions	[20, 66]
MoS <sub>2</sub> /rGO/SF nanofibers	Electrospinning method—modified Hummer's method	Induce cardiac differentiation Control self-renewal potency	[44]
CS/GO-Au scaffolds	Freeze-drying method	Improves cardiac contractility Increase electrical conductivity Restores ventricular function	[39]
GO/alginate microgels	Electrospraying	Enhanced cell viability Improve cardiac function Decrease infarction	[67]
PPy/SF nanofibers	Electrospinning	Exhibit anti-oxidant activity Mimic myocardium fibrils Exhibit contraction synchrony Showed significant electrical conductivity	[45]

immersed in the prepared PCL solution, resulting in the formation of printing ink. The Cartesian robot was used to construct PCL scaffolds containing periodic lattices. The needle of a device containing printing ink was immersed in a 90% ethanol bath and scaffolds were printed on petri plates inside the ethanol bath. *In vitro*, there was no toxicity for up to 21 days when mouse bone marrow mesenchymal stem cells (mBMSC) were seeded onto a polymer surface. According to the 3-(4,5-dimethylthiazol-2-yl)-2,5-diphenyltetrazolium bromide (MTT) and cell viability assay, cells spread on the surface of scaffold proliferate well. Also, mBMSC-seeded scaffolds were used for cartilage TE [64].

#### 4 Tissue engineering applications

It's a domain of study that deals with the development of biomimics to repair, restore, maintain and amplify or strengthen several biological functions at the level of tissue and organ [1]. Several attempts have been made in the past decades to develop NM-based scaffolds for their application in TE (Fig. 6) and we have culminated and briefly described the recent advances in the subsequent sections.

#### 4.1 Cardiac tissue engineering applications

Engineering of myocardial cells and tissues takes place using a variety of NMs functionalized or intercalated with several types of biomaterials such as chitosan (CS), silk fibroin (SF), etc. Different applications of NMs in cardiac TE are briefly discussed and summarized in Table 2 (Fig. 7). Figure 8 illustrates several strategies for electrically conductive engineered scaffolds utilizing different NMs for regeneration of cardiac tissue [103].

A widely suitable NM is GO because it possesses mechanical and electrical conductivity similar to natural heart tissue [4, 108]. Paul et al. have developed a bio-compatible and injectable fGO/DNA<sub>VEGF</sub>/GelMA (methacrylated gelatin) hydrogel for cardiac repair and vasculogenesis. Hydrogel can effectively transfect myocardial tissues, thus influencing preferable therapeutic effects and eliminating cytotoxicity. A rat model was used to justify the result with acute myocardial infarction and the hydrogel was injected into the periinfarct zone. The injected hydrogel manifested favorable effects on revascularization at the infarction site and enhanced contractile function [4, 62]. Cardiovascular diseases, including myocardial infarction and heart attack, happen due to severe loss of myocardial cells, causing abnormal electrical function. Cardiac muscles have limited regenerative capability as compared to other tissues, and when they are

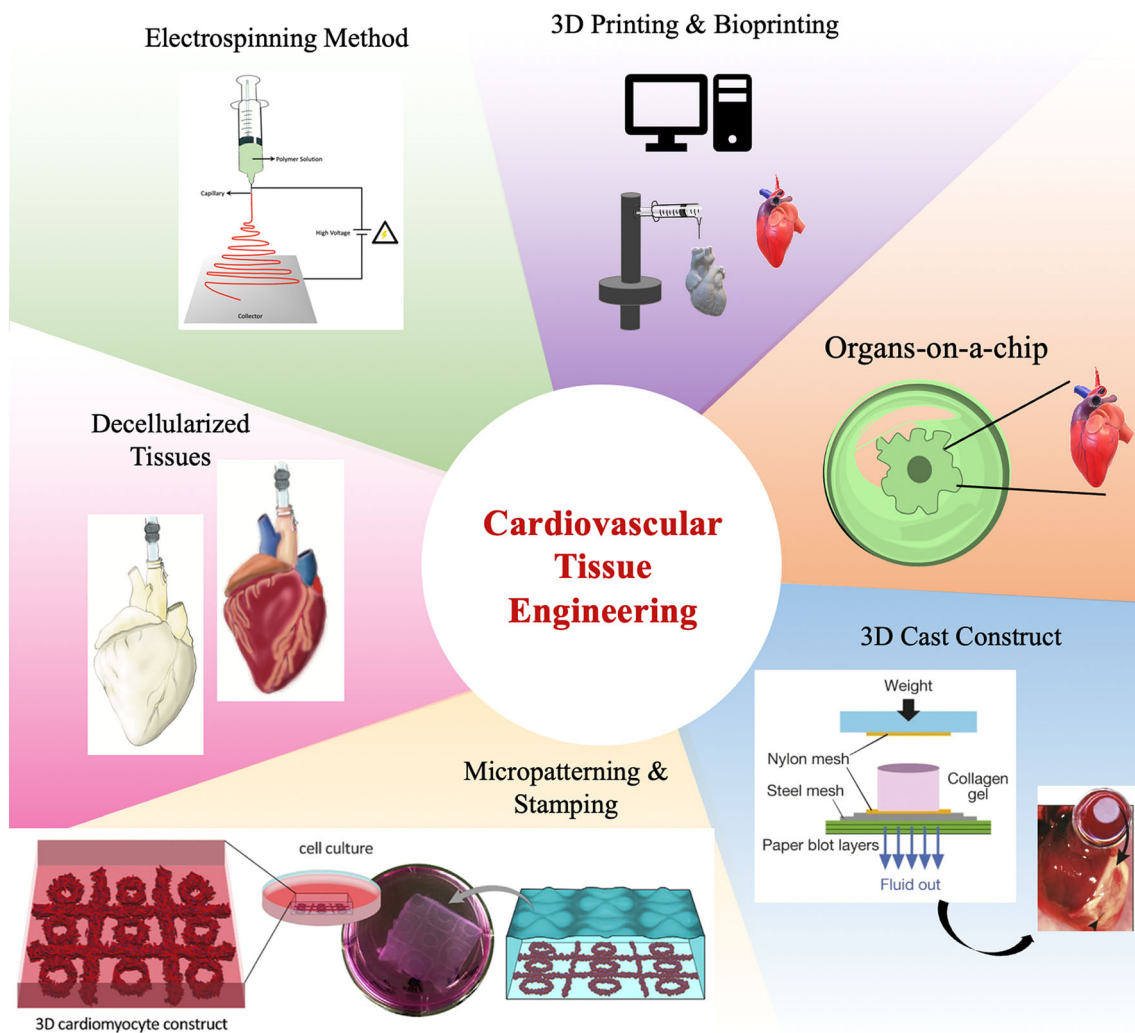


**Fig. 7** Schematic overview of cardiac tissue engineering paradigms and commonly used bioengineering approaches, including 3D printing, 3D cast construct (reconstructed from [104]), electrospinning,

organ-on-a-chip methods, micropatterning and stamping and decellularized tissues [106]

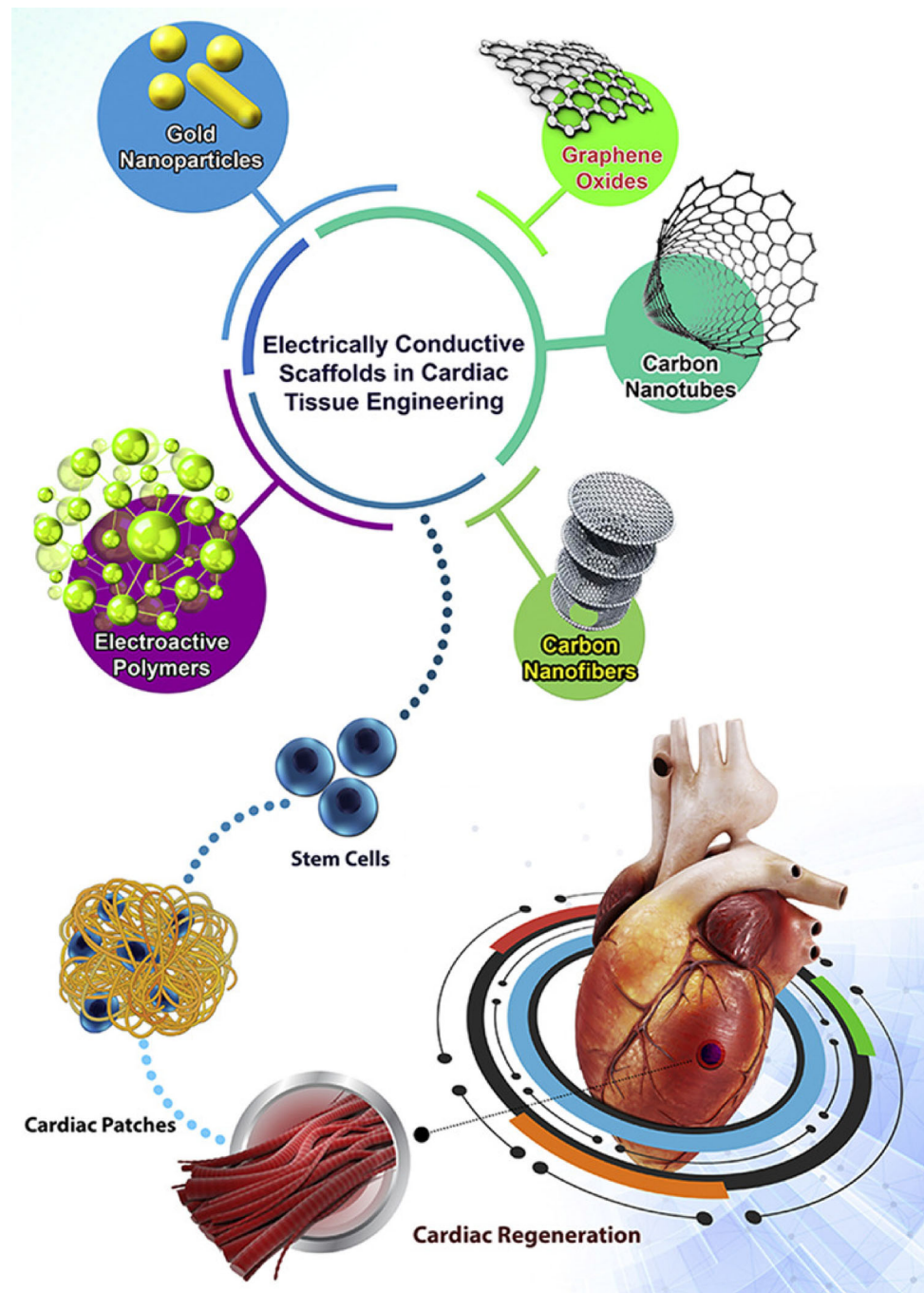
damaged, scar tissue is formed, with permanent loss of myocardial tissue [20, 109, 110].

A CS/DA/GO hydrogel has been developed by oxidizing and showing improved myocardial stem cell viability and proliferation. An amide bond was formed between CS and GO in the hydrogel. The high mechanical strength of the hydrogel was due to the nanofibrillar structure of the hydrogel that easily transfers load upon stress. Nanofibrils behave as bridges that facilitate self-healing capability. Due to aggregation formed by GO layer, which induced oxidative stress, high GO loading to hydrogel affected cell adhesion and viability, resulting in significant influences on biological and toxicological adherent cell responses [20, 65]. Fabrication of PEGylated CS hydrogel has been developed and, when dispersed with TiO<sub>2</sub> NPs, showed improved retention and adhesion of myocardial cells by the

meshwork of NPs. In hydrogels, PEG and CS are connected by H-bonding and electrostatic interaction. The aldehyde group of PEG was chemically cross-linked by the incorporation of TiO<sub>2</sub> NPs onto PEG/CS [20, 66].

Nazri et al. fabricated a SF nanofiber using MoS<sub>2</sub> and reduced GO (rGO) and then incorporated them into SF nanofibers via an electrospinning process. These nanofibers have been shown to trigger cardiac differentiation and guide self-renewal potential. In the SF/rGO hydrogel, the cells are extensively dispersed and lengthened while the cells are networked in SF/MoS<sub>2</sub> and form aligned bundles. Fabrication of MoS<sub>2</sub> and rGO in SF reinforces cardiac differentiation but doesn't affect proliferation and self-renewal capability. The density, elongation and arrangement of cells on rGO and MoS<sub>2</sub> incorporated SF scaffolds surpass those of SF nanofibers [44]. Choe et al. developed a

**Fig. 8** Different categories of nanomaterials utilized for the production of electrically conductive cardiac tissue engineering scaffolds. Reprinted with permission, [103] Copyrights © 2019 Elsevier B.V. All rights reserved



microgel composite of rGO and alginate via electro-spraying, encapsulating mesenchymal stem cells (MSCs). Further, they have enhanced cardiac maturation significantly due to ROS scavenging by the microgels. Also showed a decrease in infarction area and cardiac function improvement by the use of rGO/alginate microgels [67].

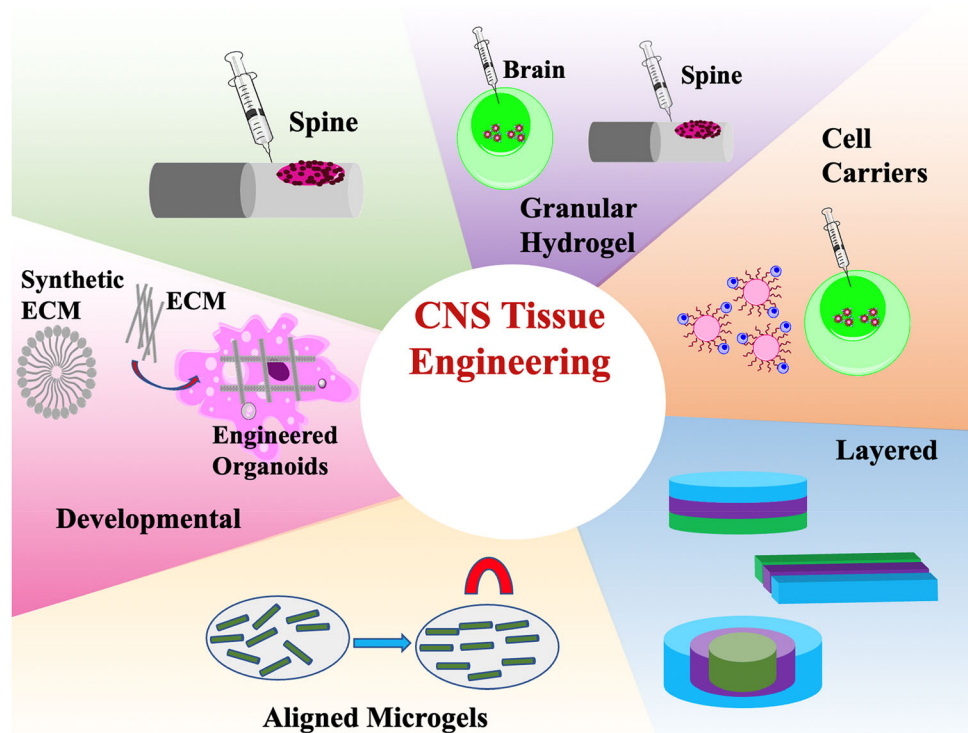
Saravanan et al. have fabricated a GO/Au nanosheet and incorporated it into a CS scaffold via the freeze-drying method. Their results demonstrate improved cardiac contractility and ventricular function restored upon implanting

the novel scaffold in the infarcted heart. It also enhances cell growth and attachment without any cytotoxicity effect. In a rat model with an isolated heart, there was an enhancement in QRS interval accompanied by increased conduction velocity and infarct region contractibility due to an enhancement in connexin level after 5 weeks of implantation of the scaffold. In the synthesis of the scaffold, Au NPs were attached to GO sheets via electrostatic interaction while an amide bond was formed between the

**Table 3** Nerve tissue engineering applications

Nanocomposite	Synthesis method	Highlights	References
TiN microelectrode arrays	IBAD/IME process	Mimic nerve tissue Enhance the longevity of implants	[68–75]
Cellulose/pyrrole monomer MWCNTs/PCL scaffold	In situ vapor phase polymerization Ionic modification followed by ultrasonic treatment	Improved adhesion and proliferation of PC12 cells Neurite growth Axonal elongation Neuron growth	[20, 54] [76, 77]
Mesoporous silica/PAMAM	Covalent attachment	Transfection efficiency Cellular uptake	[76]
Au/immobilized silica spheres	Coating method	Enhance neurite adhesion	[76]
Poly(L,D-lactide) fibers/collagen I hydrogel	Single layer-by-layer process via electrospinning method	Directed cell growth and extension of neurites Mimic cell guiding cure in CNS Enable a culture of hPSC-derived neuronal cells for a longer duration	[46]
M.SF/alginate hydrogels	Centrifugal spinning/micro-cutting method	Injectable, minimal invasive Effective nerve injury repair	[80]

**Fig. 9** Structured hydrogels in central nervous system models and therapy such as for drug delivery applications (Reconstructed from [115]), as carriers supporting cell transplantation (Reconstructed from [116]), as aligned hydrogels that guide axon growth and neurite orientation (Reconstructed from [117]), as bridging scaffolds facilitating neuronal growth across damaged tissues (Reconstructed from [118]), layered hydrogels to compartmentalize neurons thereby replicating in vivo tissue structure (Reconstructed from [119]), and instrumental in the generation of neuroepithelial cysts and organoids used as in vitro developmental models (Reconstructed from [120])



carboxylic groups of GO/Au and the amide group of CS [39].

Liang et al. have demonstrated in a recent investigation employing PPy enclosing nanofibers of SF protein that was prepared using an electrospinning method for enhancing synthetic cardiac tissue functionality. Their results demonstrate that the formed scaffold has a better ability to

mimic myocardium fibrils. Further, they showed that a PPy/SF ratio of 30:70 demonstrated contraction synchrony that could be further enhanced by external stimulation. Therefore, they proposed that PPy/SF nanofibers could potentially be used to enhance the functionality of engineered myocardium [45].

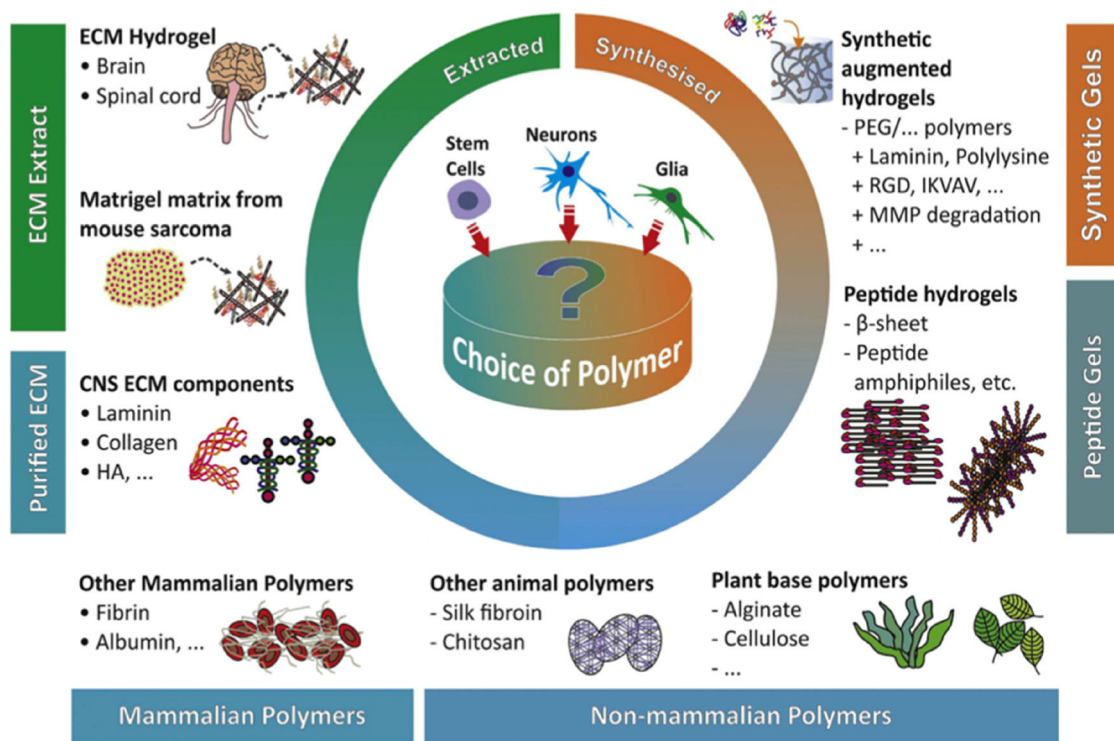
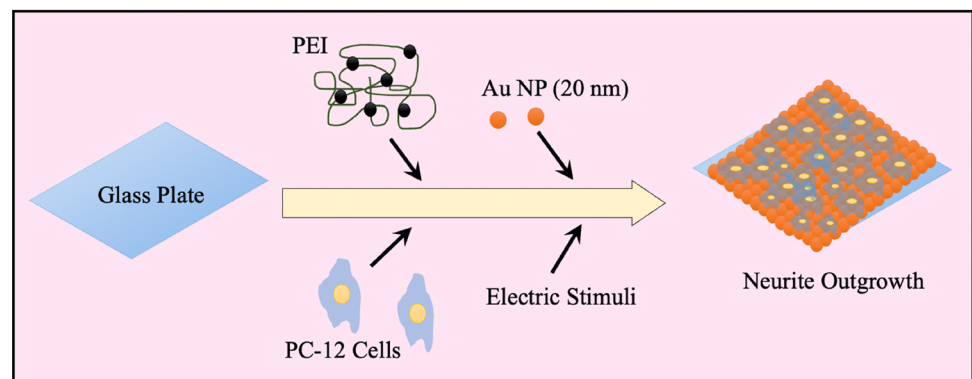


**Fig. 10** Different sources of polymer used in hydrogel preparations for central nervous system applications. ECM, extracellular matrix; HA, hyaluronic acid; PEG, poly(ethylene glycol); RGD, Arg-Gly-

Asp; IKVAV, Ile-Lys-Val-Ala-Val; MMP, matrix metalloproteinases. Reprinted with permission, [114] Copyrights © 1969, Elsevier

**Fig. 11** Schematic representation of Au NPs-coated PEI for nerve regeneration by altering electrical stimulation [122] Reconstructed from [Park JS, Park K, Moon HT, Woo DG, Yang HN, Park K-H. Electrical pulsed stimulation of surfaces homogeneously coated with gold nanoparticles to induce neurite outgrowth of PC12 cells. *Langmuir*. 2009;25:451–7]



## 4.2 Nerve tissue engineering applications

As of today, a major challenge is the regeneration of nerve tissues. In addition, there are other issues associated with nerve injuries, such as degeneration of nerves, the formation of scar tissue, and disrupted communication between cells and neurons [76]. Flecked tissues can be established at cut ends in repairing peripheral nerve injuries due to glia and hyperplasia that avert recovery of renewal nerve fibers. As a result, it is critical to use conducting hydrogels as transverse to prevent excessive connective tissue growth at

lesions [111]. In order to overcome these limitations, several NMs-based approaches have been invented as promising methods for applications of neuroengineering due to their suitable physicochemical properties and biocompatibility [76, 112, 113]. Different applications of NMs in nerve tissue architecture are briefly discussed and summarized in Table 3.

A recent study associated with the engineering of central nervous system (CNS) tissue and the commonly used hydrogels has been briefly described (Fig. 9). Further,

Fig. 10 illustrates many kinds of polymer-based materials that have been utilized for CNS tissue architecture [114].

Several other novel therapeutic approaches have materialized in the past decade. To mention a few, they are the use of graphene, nanotube-based on carbon NMs and various imaging and biosensing methods with potential action of antioxidants, ability to cross the blood–brain barriers, intrinsic photoluminescence, etc. [7]. The high-throughput screening of chemicals and neurotoxicity has been performed effectively by d'Amora and Giordani using zebra fish as a model due to its transparency, cost-effectiveness and smaller size and has led to the emergence of zebra fish animal models as a powerful tool [7, 121].

Directed delivery of nerve growth factor (NGF) and genes can be facilitated by conjugating biomolecules onto metallic NP surfaces like Ag and Au. Au NPs interact with peptide that further binds to amyloid  $\beta$  protein ( $A\beta$ ) aggregates, subsequently dissolving aggregates due to the application of local heat of Au NPs. For Alzheimer's prognosis, Au NP-based optical biosensors have been developed. Adsorption of Au NPs on positively charged cover glass with poly(ethylene)imine (PEI) resulted in better adhesion to neurites (Fig. 11). Au NPs enhance neurite outgrowth of pheochromocytoma (PC12) cells and alternating electrical stimulation that was estimated by cell viability establishment via RT-PCR and  $\beta$ -tubulin. 90% of cells survived in an altered electrical stimulation state, while 70% of cells survived with constant electrical stimulation. This is due to the generation of oxygen by the decomposition of hydrogen and water in the case of constant electrical stimulation [76, 122].

Another method is the covalent attachment of poly(amidoamine) (PAMAM) onto a mesoporous silica nanostructured surface stacked with plasmid DNA. This showed good biocompatibility, gene transfection efficiency, and cellular uptake for Chinese hamster ovarian (CHO) cells, neural glia (astrocytes) and human cervical cancer (HeLa). Due to mesoporous structure of silica nanosphere, impermeable constituents such as fluorescent dyes and pharmaceutical drugs were allowed to be enveloped in the silica channel [76]. For differentiation of stem cell-derived neuronal cells and to deliver siRNA to them, core–shell  $ZnFe_2O_4@Au$  magnetic NPs have been employed [76, 123]. The CNTs interact with the brain, which helps in the development of CNT-based devices. Because of their unique electrical properties, CNTs are viable for recording neuronal activity and stimulation. Because of electrical coupling among somatic and dendritic neuronal parts by CNTs, an increment of electrical activity in neurons. Results in MWCNTs with modified neuron growth [76, 77].

Nerve tissue lesions have been studied using several approaches and the most commercialized approach for the

treatment of nerve disorders is to implant autografts, xenografts or allografts to lesions, but this can induce a host immune-rejection reaction. In order to overcome this, the development of hydrogels can be used for nerve tissue regeneration by providing an adequate conductive environment for electrical signal exchange and conductive characteristics that promote neuronal differentiation and promotion [20].

A nanoporous cellulose gel (NCG)-PPy conductive hydrogel has been developed via in situ vapor phase polymerization of monomeric pyrrole (Py) with NCG in aqueous alkali solution and demonstrated a conductivity of 80 mS/cm. In NCG-PPy, an H-bond was formed between the -OH groups of cellulose and the -NH groups of the Py rings. NCG-PPy also showed improved or enhanced PC12 cell adhesion and proliferation, inducing neurite outgrowth, and improved biocompatibility. Under electrical stimulation, the nerve conduits have a function similar to the myelin sheath and stimulate nerve outgrowth and axon regeneration that leads to the repairment of nerve injuries [20, 54]. The fabrication of magnetic NPs along with GFs to support nerve tissue regeneration has been assessed by Pinkernelle et al. The authors functionalized iron oxide NPs, PEI-coated along with NGF, both covalently and non-covalently. Covalently bonded NGF and PEI-NPs are not able to distinguish PC12 cells that lack the biofunctionality of NGF. Non-covalent binding of NGF with PEI-NPs distinguishes PC12 cells to neuronal-like cells, hence manifesting the biofunctionality of NGF [7, 124]. Also, they assessed GF functionality using congruous or apt animal or biological models.

Graphene is the most widely used carbon-based NM. Its potential use in the regeneration of nerve tissue has been elaborated by Convertino et al. Researchers deposited epitaxial graphene on silicon carbide (SiC) via a thermal decomposition process. In analysis with PC12 cells, no cell differentiation occurred in the absence of NGF, while a significant neurite outgrowth occurred in the presence of NGF treatment on day 5. When compared to controls at differentiation of day 5, cells outgrowth graphene with an increased neurite length. Also, dorsal root ganglion neurons survive until day 17 on graphene with a dense axon network. Graphene is used as an active substrate for nerve guidance in conduit devices. Allow electrical signals to be transmitted among neurons that make external stimulation feasible to increase regeneration of axon [7, 125].

A  $\gamma$ -aminobutyric acid (GABA) microarray probe has been developed by Hossain et al., which consists of two biosensors constructed by glutamate (Glu) oxidase and GABASE enzymes used in the detection of Glu and GABA, respectively. They have successfully shown that the invention of the GABA probe could be a novel approach and could be implemented in brain disorder

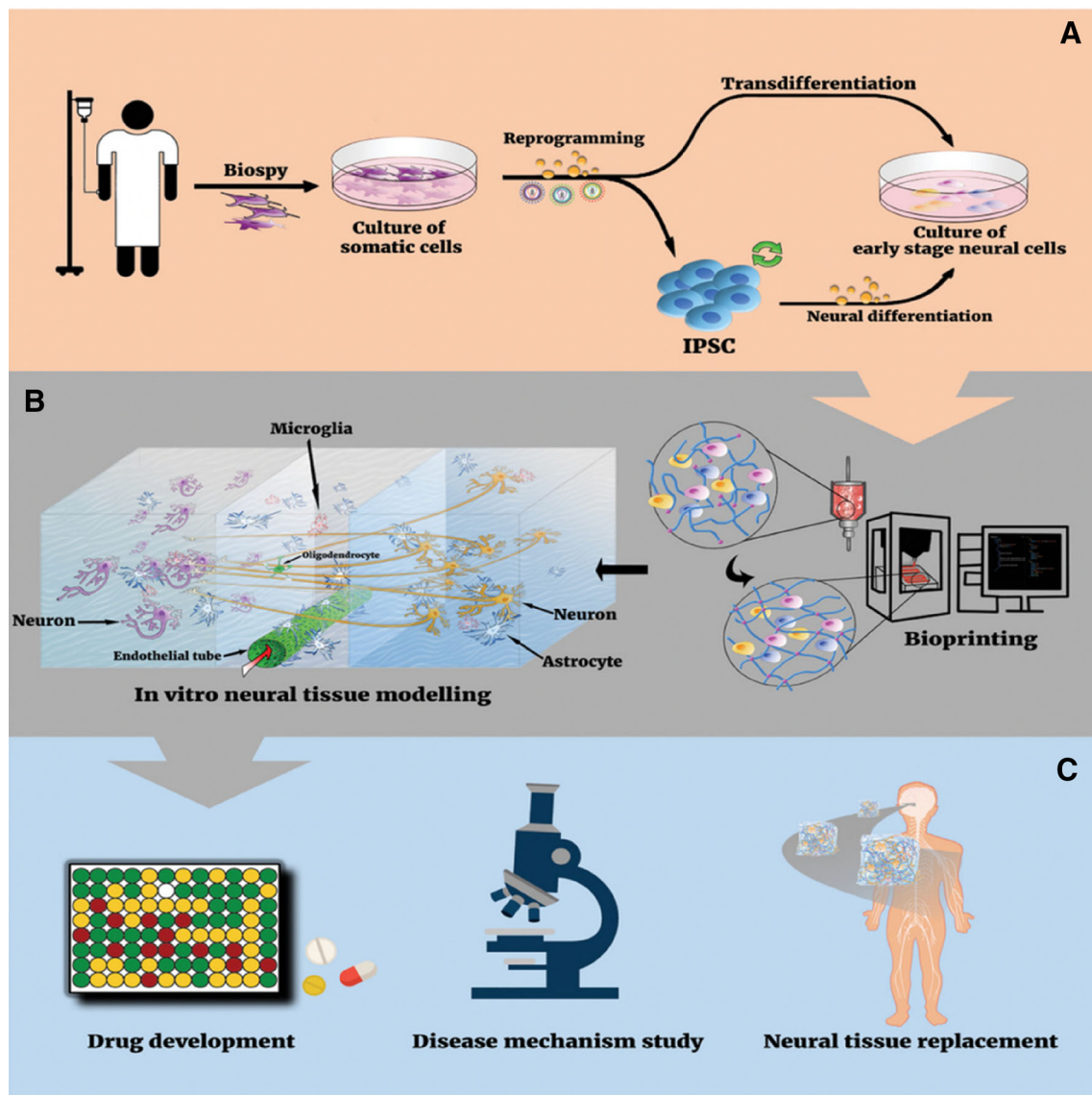


**Fig. 12** Schematic representation of personalized *in vitro* bioprinted neural tissue models. **A** Derivation of neural cells through direct cell reprogramming or induced pluripotent stem cells approach. **B** Bioprinting with patient-specific neural cells to generate neural tissue

models. **C** Intended applications with bioprinted neural tissue models. Reprinted with permission, [128] Copyrights © 2020 The Authors. Published by WILEY-VCH Verlag GmbH & Co. KGaA, Weinheim

studies amalgamating the involvement of GABA and Glu signaling. The key benefits were that the location of the microelectrode array along with the shank at numerous depths in the brain allows GABA and Glu sensing. It concurrently senses neurochemicals and field potentials. That's impossible with the latest neurochemical strategies [7, 68, 126, 127].

Recent studies reveal that intracortical microelectrodes (IME) can be utilized to enhance and mimic biological tissue, especially nervous tissue and have been extensively studied. Nano-architectural approaches examine the surface of the implants and several approaches have been discussed by Kim et al. to improve IME biocompatibility

and improve the quality and longevity of the implant [68–71]. A possible substitute to the titanium nitride (TiN) deposition approach has been invented by Ryyänen et al. where they have implemented a process based on ion beam assisted e-beam deposition (IBAD) for TiN microelectrode arrays (MEAs) fabrication. The authors cultured human pluripotent stem cell (hPSC)-acquired neurons in Brain-Phys (BPH) and neural differentiation medium (NDM). They support the genesis of MAP2 and  $\beta$ -tubulin-positive neural networks with synaptophysin expression within 12 days. The neuronal networks in BPH were denser than in NDM. The significant enhancement was found in the active electrode percentage in the case of BPH as compared

**Table 4** Bone tissue engineering applications

Nanocomposite	Synthesis method	Highlights	References
PEG-GO/PPF	Sonication and thermal curbing	No toxicity for human dermal fibroblasts	[4, 81]
GO/CS/nHAP	In situ crystallization	Endogenous bone repair	[4, 82]
BP nanosheets/GelMA nanocomposite	Coating method	Bone regeneration Release of calcium-free phosphate Promote mineralization	[4, 9]
BP/natural polymers	Coating method	Bone regeneration	[4, 78]
Au/photo-curable gelatin hydrogel	UV-induced crosslinking	Bone regeneration Promote osteogenic differentiation of MSCs	[20, 42]
GO-BP scaffold	3D printing, ammonolysis, coating	Enhance bone mineralization and differentiation Bone regeneration	[4, 79]
GO/CS/PVP	Electrospinning method—modified Hummer's method	Possess good mechanical strength The efficient wound closure rate	[47]
GO/PMMA/PLC/FA	Dry mechanochemical process followed by mixing	Mimic osteoblast cells Act as bone fillers in orthopedic surgeries	[83]
GO/CS/HA containing osteogenesis inducing drug SV	Electrospinning method—modified Hummer's method	Increase in osteogenesis and mineralization Exhibit good biocompatibility	[48]
CNT/HA	CVD and sol-gel method	Mimic osteoblastic and fibroblast cells	[59]
CNT/PVA	Freeze-drying method	Mimic osteoblast cells	[40]
CNT/3D collagen scaffold/ $\beta$ -tricalcium phosphate	Pulverization followed by incorporation in a collagen scaffold	Mimic fibroblast cells	[84]
CNT/PBAT fibers	Electrospinning method	Mimic MG63 osteoblast-like cells	[49]
CNT/surface-modified PCL/PLA scaffold/insulin-like GF I	Photo-immobilization technique	Mimic rBMSCs Low toxicity <i>in vivo</i> studies Exhibit anti-senescence functionality	[85]

to NDM. Cells cultured in MEA types was unsuccessful as neural networks started to disclaim and form clumps after two weeks and experiment termination was initiated within 3 weeks of the experiment duration [72–75].

Another method developed for use in neuroengineering is the single layer-by-layer electrospinning of poly(L, D-lactide) fibers with collagen I hydrogel. The results using this method have shown directed growth and extension of neurites. Also, this hydrogel nanocomposite mimics the cell guiding cues in the CNS and enables the culturing of hPSC-derived neuronal cells for a longer duration [46]. Recently, Qiu et al. have demonstrated the emerging role of bioprinting for the development of 3D neuronal models. Figure 12 illustrates the bioprinted model for a 3D neuronal *in vitro* model for neuronal tissue architectural application and biomedical intervention [128]. In a recent investigation conducted by Ghaderinejad et al., magnetic

PCL and superparamagnetic iron oxide NPs (SPIONs) were spun centrifugally to form magnetic short nanofibers (M.SF) via a micro-cutting approach. Eventually, these M.SFs were incorporated into alginate hydrogels. Further, the hydrogel with oriented M.SF was encapsulated into olfactory ecto-mesenchymal stem cells (OE-MSCs) and exhibited viability of cells even after 7 days. Furthermore, it was shown to increase neural differentiation after 14-day induction. Altogether, they proposed that injectable M.SF@alginate hydrogels could be a potential and less invasive strategy for neural tissue regeneration [80].

### 4.3 Bone tissue engineering applications

Engineering of hard (bone) tissues takes place using a variety of NMs functionalized or intercalated with several



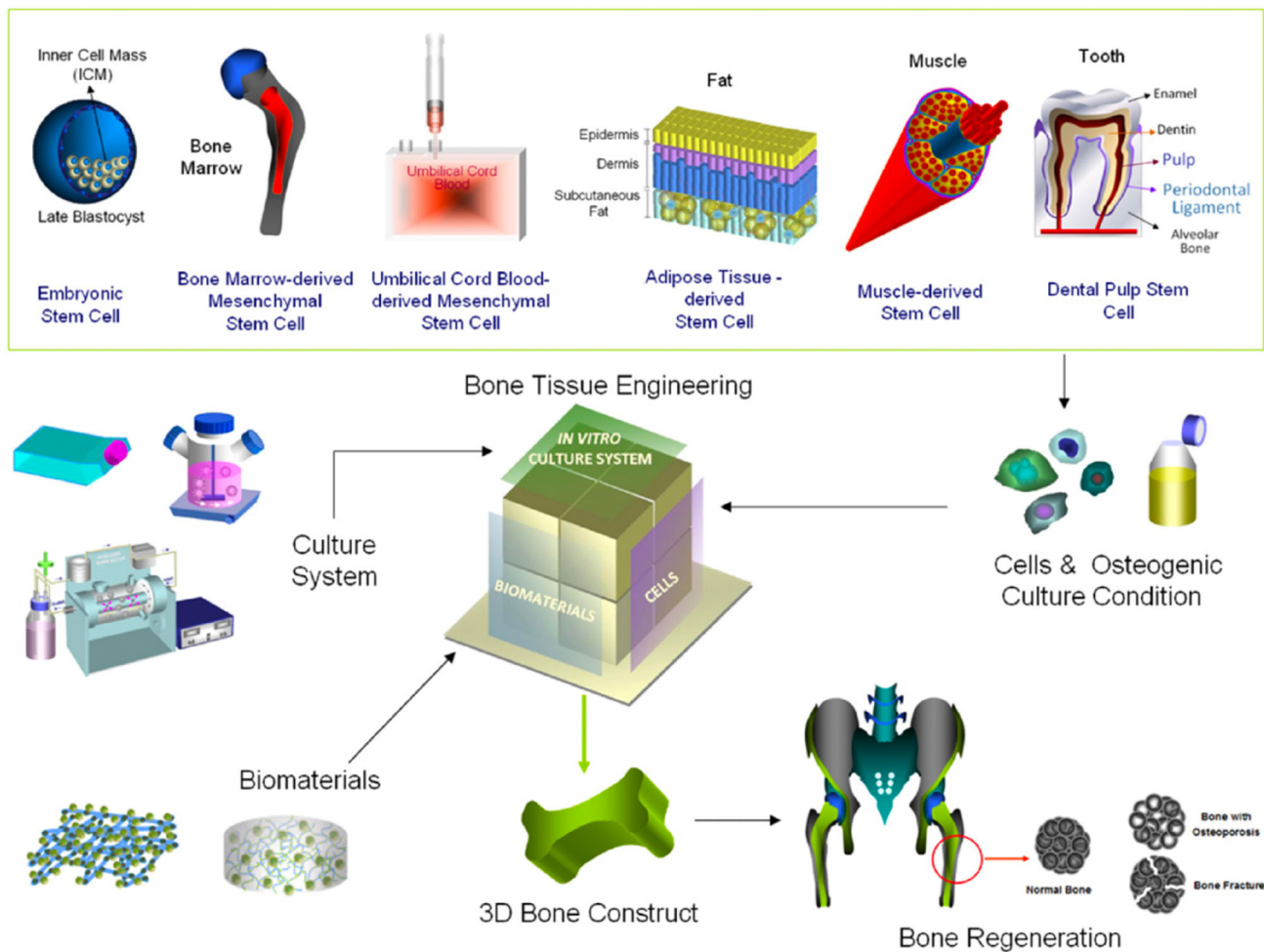


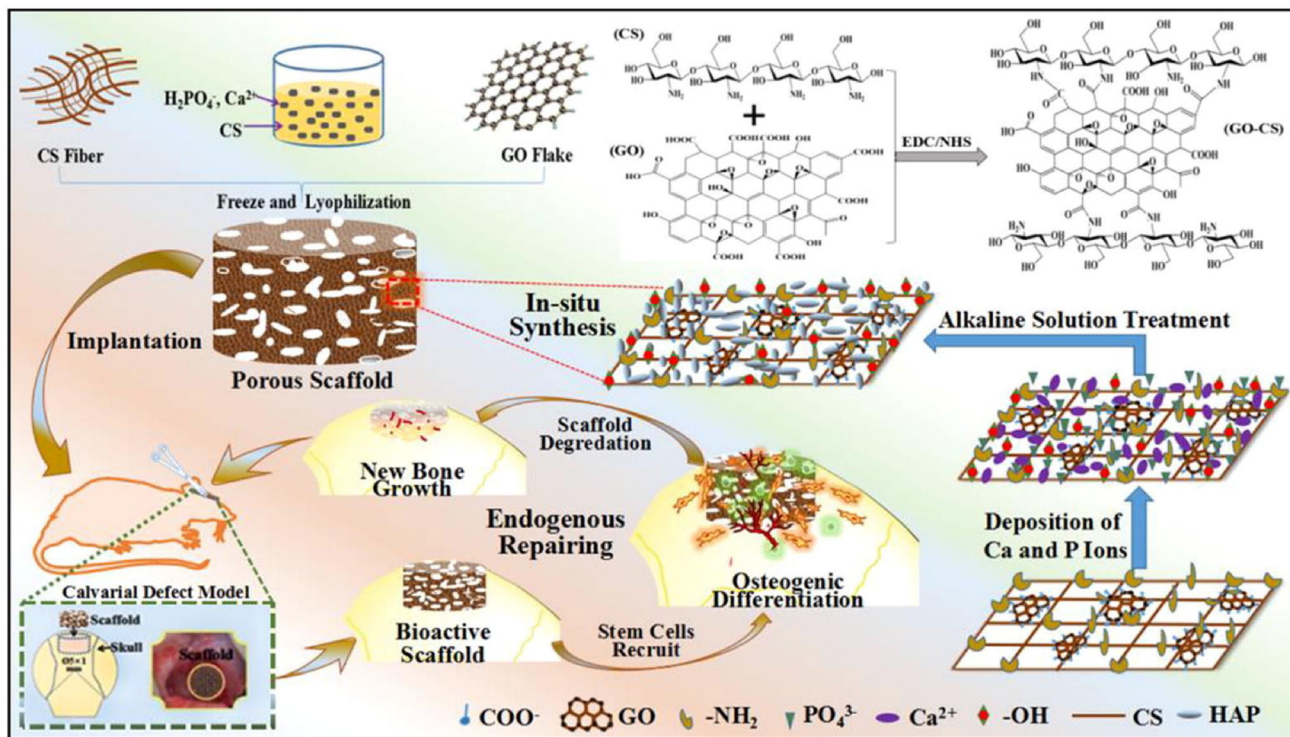
**Fig. 13** Stem cell-based bone tissue engineering. Reprinted with permission, [129] Copyrights © 2006, IOP Publishing, Ltd

types of biomaterials. Different applications of NMs in bone TE are briefly discussed and summarized in Table 4. Stem cells are an important factor for potential implementation in bone tissue architecture and regeneration (Fig. 13) [129].

GO could be used as a potential NM as it has less cytotoxicity and high biocompatibility. Similarly, thermal curing and sonication have been used to create nanocomposites such as poly(propylene fumarate) (PPF) with PEGylated GO (PEG-GO). In PEG-GO, the hydroxyl and carboxylic groups of GO formed an H-bond with the -OH group of PEG. Results showed an increase in GO concentration could increase surface roughness, thermal stability, uptake of water and hydrophilicity. Also showed no toxicity to human dermal fibroblasts. The results revealed that the bio-acidic effect was stronger for Gram-positive (*Staphylococcus aureus* and *Staphylococcus epidermidis*) than Gram-negative (*Pseudomonas aeruginosa* and *Escherichia coli*) microorganisms. GO nanosheets form hydroxyl radicals that attack bacterial cell wall peptide

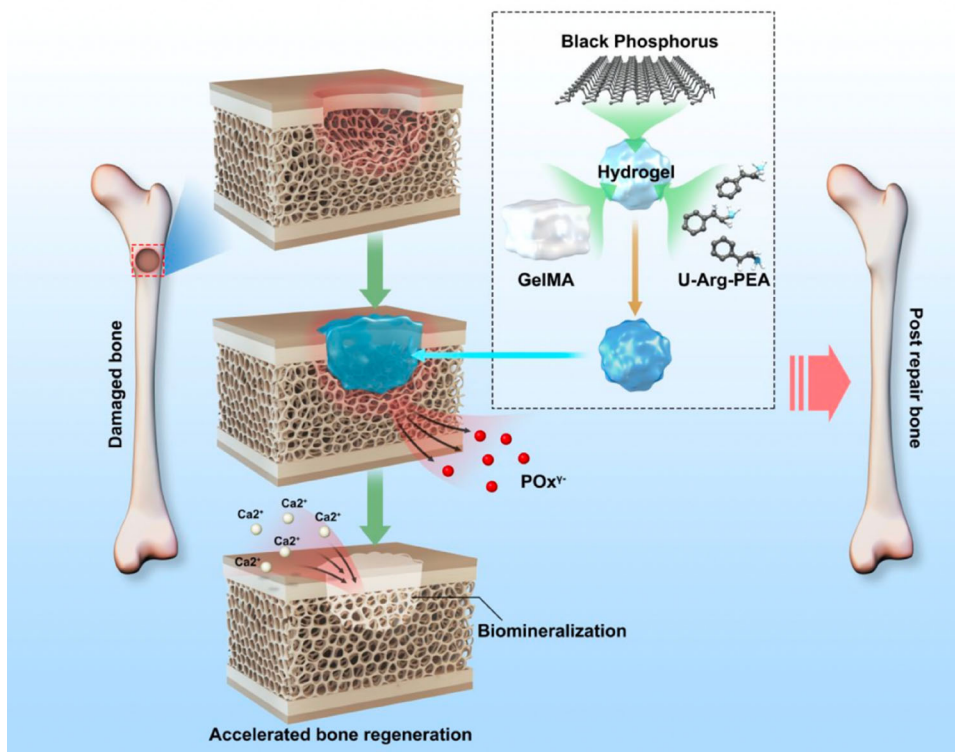
linkage and cellular component (proteins, DNA and lipids) destruction that results in the destruction of bacteria [4, 81].

Zhao et al. fabricated a GO/CS/nanohydroxyapatite (nHAP) structural scaffold via a one-step in situ bionic technique (Fig. 14). In scaffold, the carboxyl radical of GO electrostatically interacts with the amine group of CS to prevent the material from collapsing quickly in physiological fluid. Scaffolds were ideal for nutrient exchange, metabolic by-products, and cell growth and cohesion due to their rough surface, porous structure, high stability, and low positive potential value. The stability of scaffolds was enhanced by GO and that resulted in the neonatal tissue merging completely with the damaged area. The defects were filled with newly born tissue that revealed an integrated structure with endemic bone in scaffold groups. This is due to the synthesized method of scaffold, which increases the biocompatibility and interfacial bioactivity between the scaffold and endemic tissue that is embedded *in vivo*. 0.09% GO/CS/nHAP scaffolds showed exceptional bone renewal potential. Scaffolds were produced by



**Fig. 14** Fabrication of GO/CS/nHAP scaffold and process of endogenous bone repair. Reprinted with permission, [82] Copyrights © 2019 Elsevier B.V. All rights reserved

**Fig. 15** Bone regeneration using black phosphorous-based hydrogel. A 3D hydrogel platform follows a new strategy that encapsulates black phosphorous nanosheets can capture calcium ions to accelerate biomineralization in a bone defect and enhance bone regeneration. Reprinted with permission, [9] Copyright © 2019, American Chemical Society



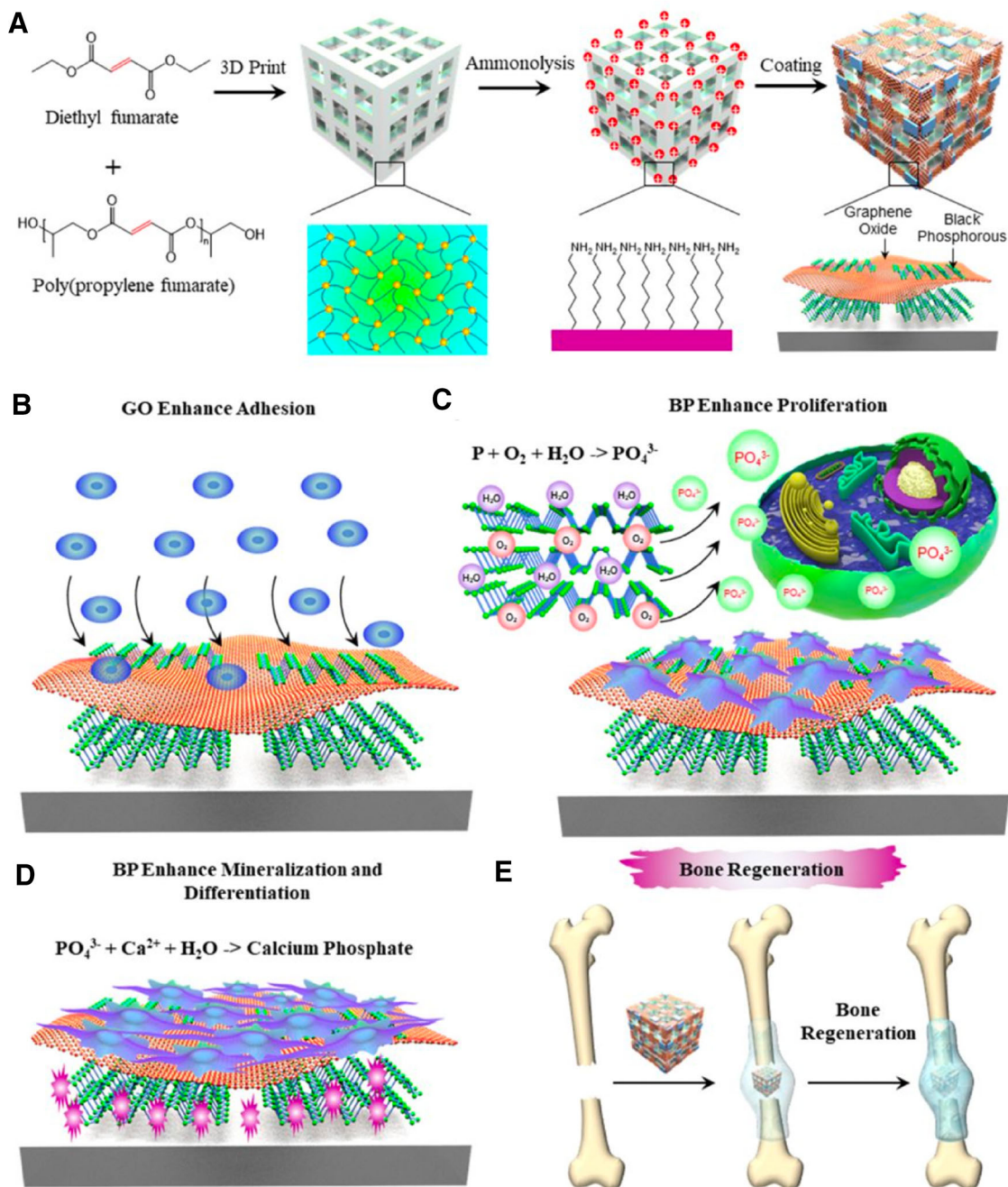


**Fig. 16** A Schematic representation of the fabrication process of 3D printed scaffolds functionalized with 2D graphene oxide and black phosphorous nanosheets. **B** Graphene oxide nanosheets enhance cell adhesion to the surface of the scaffolds. **C** Black phosphorous nanosheets release phosphate groups as they degrade, which enhance the proliferation of pre-osteoblasts. **D** Phosphate groups released from

black phosphorous nanosheets also enhance scaffold mineralization and cellular differentiation, making this approach an attractive option. **E** Schematic demonstration of 2D materials functionalized 3D scaffolds for bone tissue engineering applications. Reprinted with permission, [79] Copyright © 2019, American Chemical Society

endogenous stem cells in situ for damaged areas and eased proliferation and differentiation, promoting endogenous bone renewal [4, 82].

Materials for bone TE must possess high mechanical strength [20, 130]. So, in order to mimic bone tissue, the

mechanical strength of hydrogels must be improved as they currently possess low mechanical strength. For bone tissue regeneration, the most promising material is Au NPs as they promote mesenchymal stem cell (MSC) osteogenic differentiation [20, 42]. A biodegradable hydrogel using

**Fig. 17** Therapeutic hydrogel fabrication via black phosphorous nanosheets and natural polymer precursor [78] Reconstructed from [Miao Y, Shi X, Li Q, Hao L, Liu L, Liu X, et al. Engineering natural matrices with black phosphorus nanosheets to generate multi-functional therapeutic nanocomposite hydrogels. *Biomater Sci.* 2019;7:4046–59]

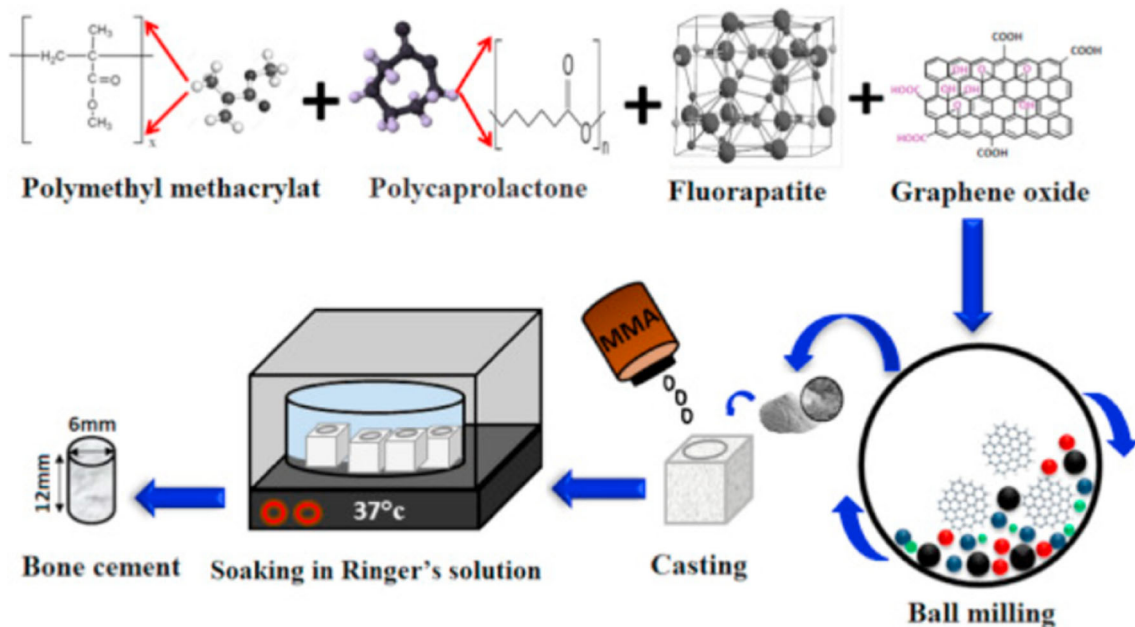
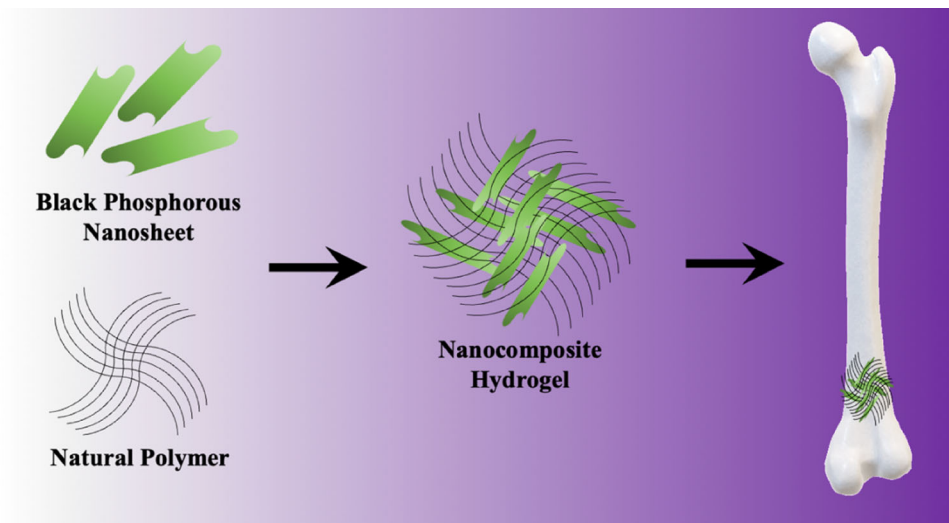


**Fig. 18** Schematic representation of formation of PMMA/PCL/FA/GO based bone cement. Reprinted with permission, [83] Copyrights © 2018 Elsevier Ltd. All rights reserved

Au NPs through UV-induced chemical cross-linking has been developed and showed regeneration of bone tissue. Au NP hydrogel exhibits significant enhancement in bone proliferation, activity, and formation [20].

Bone regeneration is facilitated by the proliferation and differentiation of osteogenic cells, which can be achieved by amalgamating black phosphorous (BP) nanosheet with hydrogel scaffolds leading to better mechanical properties and also cause the release of calcium-free phosphorous (Fig. 15). The BP nanosheets photo-responsively degraded into phosphate ions and trap calcium ions to fast-track biomineralization in bone defect *in vitro* that leads to enhance the regeneration of bone. After the implantation of

hydrogel in rabbit, medullary cavities and vessels appeared in newly formed tissue after 8 weeks that shows the formation of bone. Mature bone with successive structure distinguished in group with hydrogels within 12 weeks that indicating the complete healing of defect after addition of BP nanosheets as extra phosphorus [4, 9].

Another approach is to enhance osteogenic potential by altering the surface of the scaffold through GO and BP coating (Fig. 16). Cell adhesion and protein adsorption are improved by the addition of GO, which leads to an enhanced surface area of scaffolds, while the addition of BP leads to a continuous release of phosphate as material is degraded, which results in stretching of cell shape and

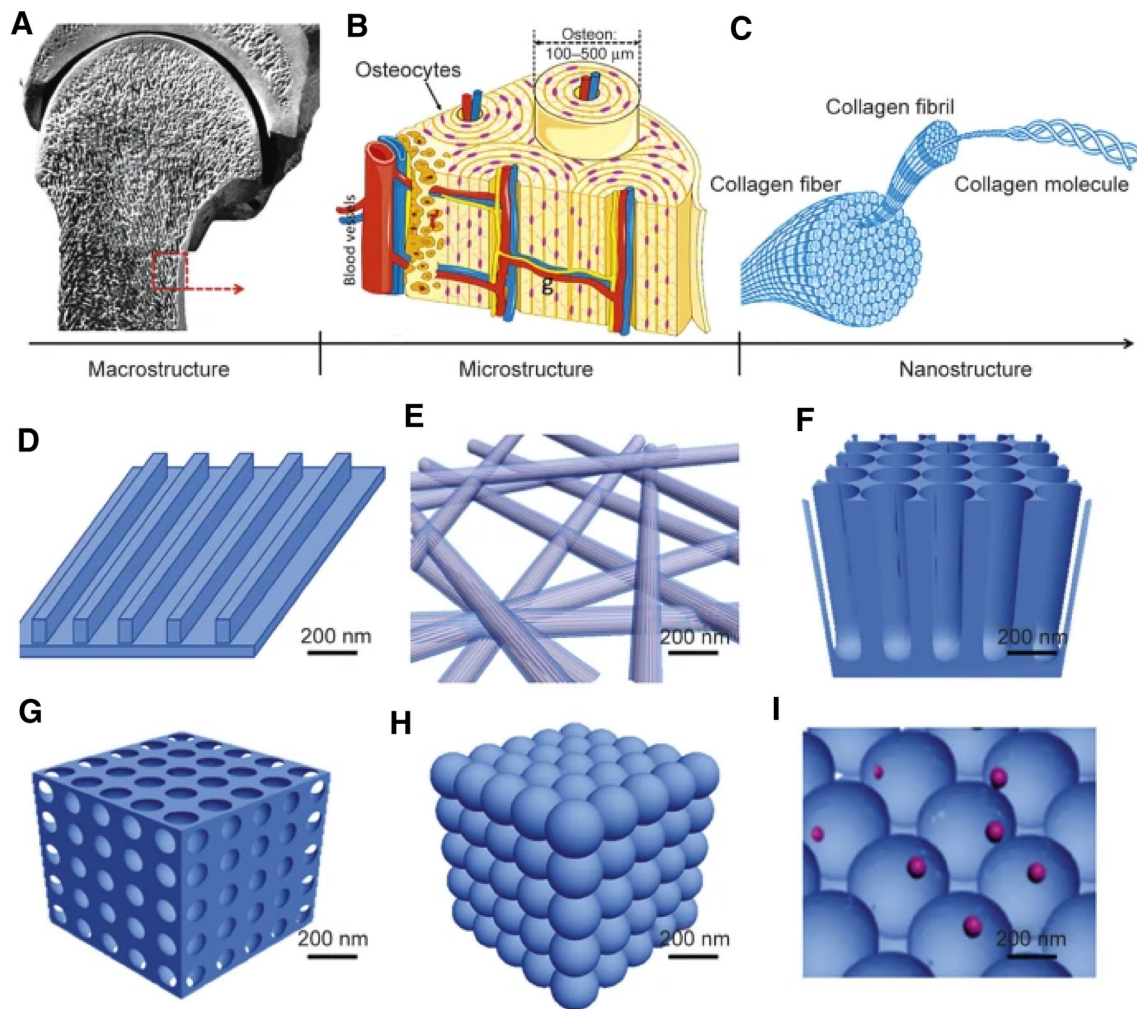


**Fig. 19** The microstructure and nanostructure of bone and the nanostructured material used in bone regeneration. **A** At the macroscopic level, bone consists of a dense shell of cortical bone with porous cancellous bone at both ends. **B** Repeating osteon units within cortical bone. In the osteons, 20–30 concentric layers of collagen fibers, called lamellae, are arranged at 90° surrounding the central canal, which contain blood vessels and nerves. **C** Collagen

fibers (100–2000 nm) are composed of collagen fibrils. The tertiary structure of collagen fibrils includes a 67 nm periodicity and 40 nm gaps between collagen molecules and increase the rigidity of the bone. Nanostructures with features of **D** nanopattern, **E** nanofibers, **F** nanotubers, **G** nanopores, **H** nanospheres, and **I** nanocomposites with structural components with a feature size in the nanoscale. Reprinted with permission, [131] Copyright © 2015, The Author(s)

cellular filament formation around edges. It also releases phosphate as an osteoblast differentiation facilitator that induces cell osteogenesis. Hence, proliferation, cell attachment, and differentiation were attained on BP-GO fabricated scaffolds [4, 79].

Miao et al. developed a composite hydrogel (BP-Gel) and showed bone regeneration *in vitro* and *in vivo* (Fig. 17). The BP nanosheet is degraded when it interacts with water and oxygen, which leads to the release of  $\text{PO}_4^{3-}$  ions. The released  $\text{PO}_4^{3-}$  ions are bound with  $\text{Ca}^{2+}$  ions obtained from osseous tissues, which results in the generation of a bone-like  $\text{Ca}^{2+}$ - $\text{PO}_4^{3-}$  matrix that is favorable for osteointegration and bone renewal. Also, hydrogel prevents wound infection (treatment of osteosarcoma) and shows performance in NIR photothermal to eliminate

bacteria and cancer cells. It also enhances cell growth and supports osteogenic differentiation *in vitro* of hMSCs without osteo-inductive factors and enhances the regeneration of bone *in vivo* [4, 78].

Another strategy is the fabrication of GO using a modified Hummer's method and incorporating it into a nanofiber composite of CS and polyvinyl pyrrolidone (PVP) via electrospinning. The results showed enhanced mechanical strength and an effective wound closure rate. When compared to a control, 1.5% GO membrane resulted in a faster wound closure rate *in vivo* (in rat) [47]. Pahlevanzadeh et al. developed a novel casting method for functionalizing GO with poly(methyl methacrylate)-PCL (PMMA-PCL) polymer and fluorapatite (FA) (Fig. 18). In this, graphene formed a hydrogen bond with the polymer chains. The

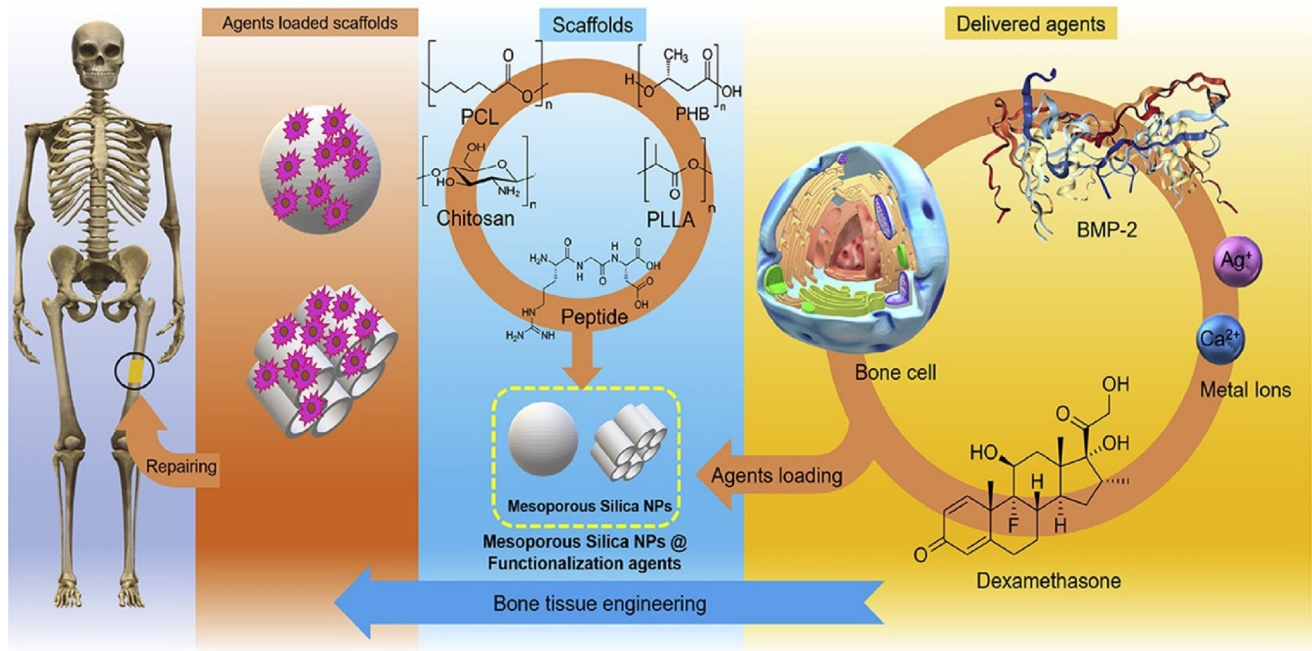
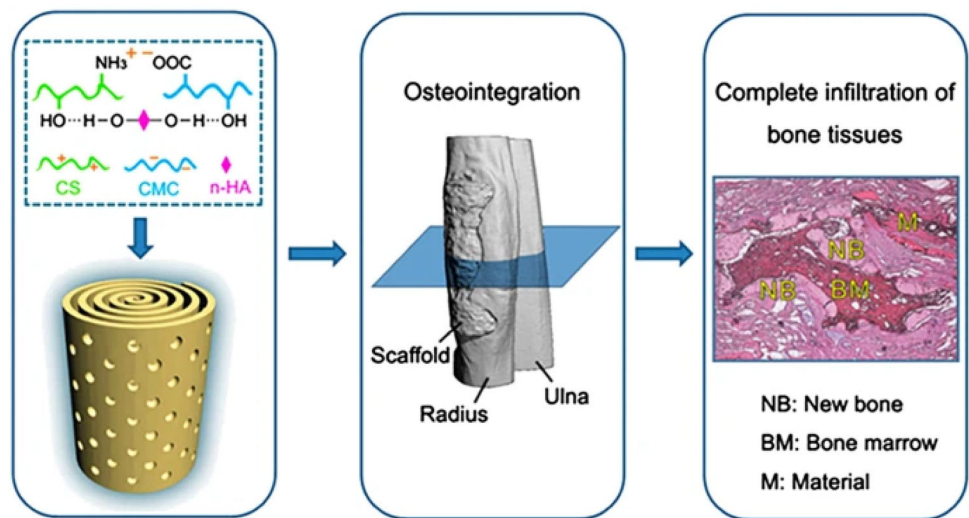


**Fig. 20** Mesoporous silica-based nanomaterials as scaffold in bone tissue engineering applications. Reprinted with permission, [132] Copyrights © 2019 Elsevier B.V. All rights reserved

**Fig. 21** Biomimetic spiral-cylindrical scaffold based on hybrid chitosan/cellulose/nano-hydroxyapatite membrane. Reprinted with permission, [133] Copyright © 2016, The Author(s)



elastic modulus and yield strength were enhanced with the addition of FA to the polymer but reduced elongation, while the addition of GO enhanced elongation, tensile strength, cell viability, and proliferation after 7 days of culture. Also, PMMA-PCL/FA/GO has been shown to mimic osteoblast cells and in orthopaedic surgeries, they act as bone fillers. The osteoblast cells adhered and outspread on the bio-ceramic surface, as apatite-like film generation and  $\text{Ca}^{2+}$  ion production from calcium phosphate improved cell adherence and proliferation [83].

Unnithan et al. have fabricated a GO/hyaluronic acid (HA)/CS-based bioactive nanocomposite scaffold along

with simvastatin (SV) via a lyophilization technique, an osteogenesis-inducing drug. In the nanocomposite, an amide bond was formed between CS-HA and GO. The carboxylic functional groups attached to GO enhance the interaction of GO with CS and HA, which constructively starts the widespread nucleation of HA within the scaffolds. The addition of GO exhibits significant enhancement in osteogenesis and mineralization. Also, the presence of GO has improved the mechanical strength and it possesses excellent biocompatibility as a bone scaffold. The osteogenesis in both *in vitro* and Alizarin Red assay tests was enhanced with 1% SV-loaded scaffolds. The bioactivity of

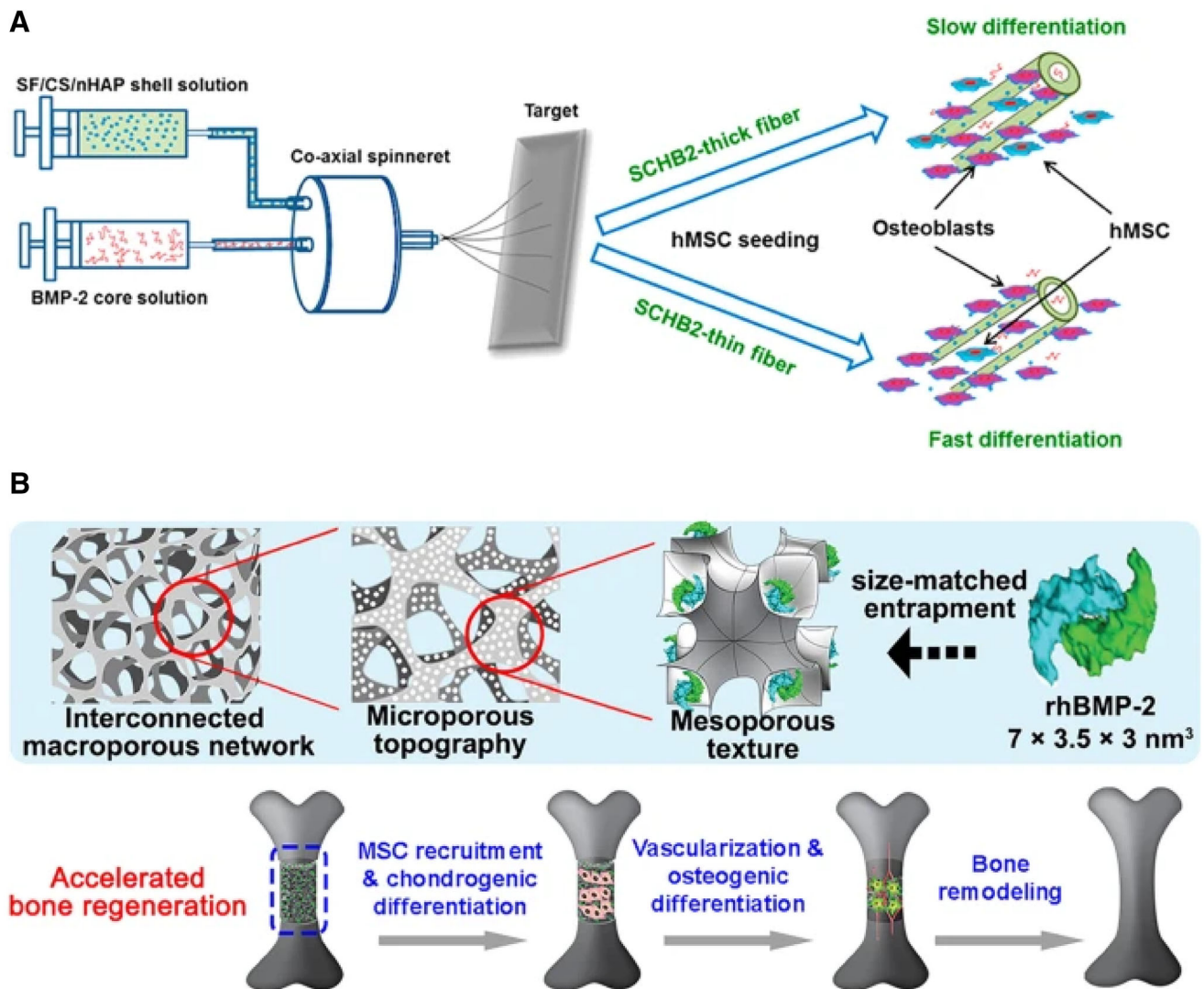


**Fig. 22 A** Preparation of SCHB2-thick and SCHB2-thin NFMs through coaxial electrospinning and their influence on hMSCs. Reprinted with permission, [134] Copyright © 2015, American Chemical Society. **B** Tri-modal macro/micro/nano-porous scaffold loaded

with rhBMP-2 for accelerated bone regeneration. Reprinted with permission, [135] Copyright © 2015 Acta Materialia Inc. Published by Elsevier Ltd. All rights reserved

the scaffold and its capability to increase apatite layer nucleation and enable integration of the scaffold into the implant site [48].

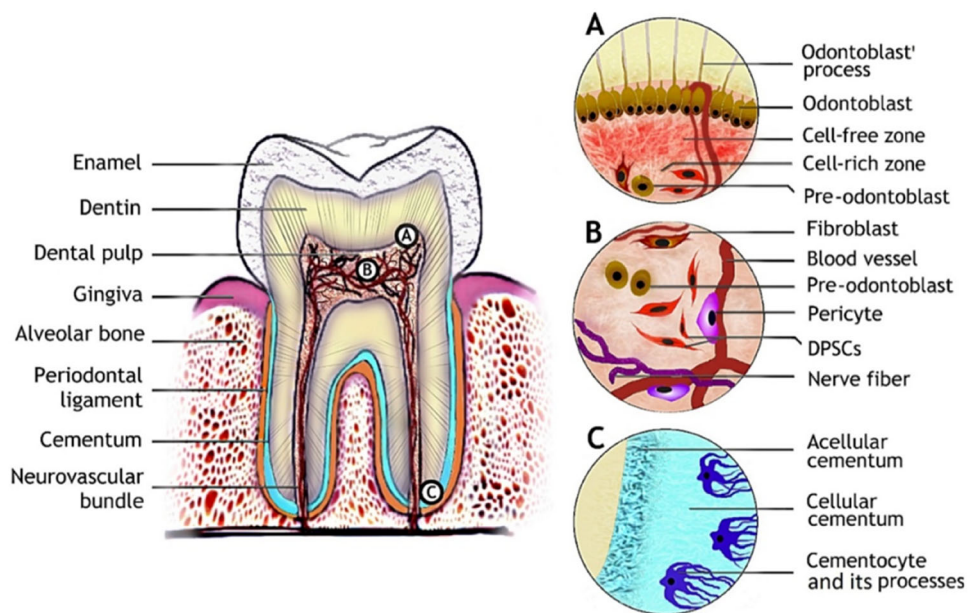
The composition of bone mainly comprises of collagen (organic) and hydroxyapatite (inorganic) with a hierarchical arrangement. Figure 19 illustrates the structure of bone at macro-, micro- and nano-structural levels along with the NMs used for bone regeneration [131]. Furthermore, silica NMs have been widely explored due to their ability to enhance bone cell growth and delivery of encapsulated biologically active molecules in mesopores (Fig. 20) [132].

Li et al. have developed HAP composites by reinforcing CNTs via a double in situ process, i.e., by combining CVD for synthesizing CNTs in HAP powder and then using a sol-gel method for further encapsulation of CNTs. Due to

excellent biocompatibility, this has shown to enhance mechanical strength and exhibit significant improvement in the proliferation of fibroblasts. This shows high potential in bone TE applications.  $\text{Ca}^{2+}$  ions through electrostatic interaction adsorb onto the surface of CNTs followed by reaction with  $\text{PO}_4^{3-}$  ions that leads to the formation of HAP on the CNT surface via electrostatic interaction, which is responsible for the high flexural strength of the scaffold [59].

Kaur et al. developed a nanocomposite scaffold employing PVA and CNTs via the freeze-drying method. They showed that the fabricated scaffold mimics osteoblast cells and also increases the mechanical strength by many folds due to varying concentrations of CNTs. Further, it's a favorable scaffold for amplifying bone tissue renewal. For

**Fig. 23** Tooth structure and dental tissues with the respective stem cell populations. **A** The odontoblast niche is bordering dental pulp beneath the dentin with odontoblast processes projecting towards enamel. **B** Diverse cell populations are found in dental pulp, DPSCs, which can give rise to odontoblasts. **C** Cementocytes are residing in the lacunae of cellular cementum at the root apex with their cellular processes projecting towards the periodontal ligament. Reprinted with permission, [137] Copyrights © 2016, MDPI Journals



proliferation and differentiation of osteoblast cells, 1 wt% CNT in the scaffolds provided the best result, while 1.5 wt% CNT reduced the mechanical strength and *in vitro* cell growth. The scaffold's ability was to form a bond with bone via bone-like apatite layer generation on the surface upon implantation. The apatite layer was formed by the deposition of  $\text{Ca}^{2+}$  ions on carboxyl groups, followed by  $\text{PO}_4^{4-}$  ions. Also, carboxylic and hydroxyl functional groups on the CNTs surface adsorb proteins by electrostatic and van der Waals interactions [40]. A spiral-cylindrical scaffold using a hybrid membrane of sodium carboxymethyl cellulose was arranged in a concentric manner for osteointegration and bone repair (Fig. 21). Nanofibrous membrane (NFM) preparation has been illustrated with BMP-2 as the core and silk fibroin/chitosan/nano-hydroxyapatite (SF/CH/nHAP) as the shell via electrospinning as an excellent bone scaffold (Fig. 22) [133].

Miyaji et al. have developed a method using MWCNTs and  $\beta$ -tricalcium phosphate ( $\beta$ -TCP) NPs and then a mixture of MWCNTs/ $\beta$ -TCP NPs was incorporated into a collagen scaffold and shown to mimic fibroblast cells [84]. Rodrigues et al. have fabricated MWCNT/poly(butylene adipate-co-terephthalate) (PBAT) fibres via electrospinning methods. They showed enhanced mechanical strength and mimicked MG-63 cells' osteogenic differentiation. There were sequential cellular events that arise when cells attach to the surface of biomaterials. Startlingly, cells did attachment and proliferation, followed by differentiation to synthesize collagen and proteins, as well as their own *in vitro* mineralization in specific medium. The best results were obtained with 0.5 wt% CNT/PBAT [49]. Chen et al. created surface-modified poly(caprolactone)-poly(lactic

acid) (PCL-PLA) scaffolds with CNTs and insulin-like growth factor I via a photo-immobilized method, and demonstrated low toxicity *in vivo*, amplify bone healing and have anti-senescence functionality by downregulating MSC protein associated with senescence and upregulating protein associated with bone morphogenesis [85].

#### 4.4 Dental tissue engineering applications

Dental disorders and injuries, along with increased life expectancy, have led to a significant demand for dental tissue regeneration [136]. The self-regeneration ability of dental issues is very limited or almost nil [136, 137]. The complex architecture of dental tissues, that is, the presence of a defined amount of HAP crystals and matrix proteins such as lacunae, accounts for suitable replacement material that must be biocompatible and wear-resistant. However, there are already known indications for tooth formation and regeneration that have been diligently studied and may require further innovation in the future [137, 138]. Figure 23 demonstrates the complexity of a mature tooth that consists of hard non-vascularized tissues and soft vascularized dental pulp [137].

For regeneration of dental tissue, scaffolds and biomolecules are crucial templates and act as attachment sites for regenerative cells possessing the ability to differentiate. In addition, the scaffold has application as a delivery approach for drugs or GFs, which could improve the potential for regeneration of dental tissue [137, 139–141].

To date, several stem cells (SCs) have been widely used, such as embryonic stem cells (ESCs), bone marrow mesenchymal stem cells (BMSCs), and other tissue-specific SCs. SCs have the potential to produce 3D tissue-like



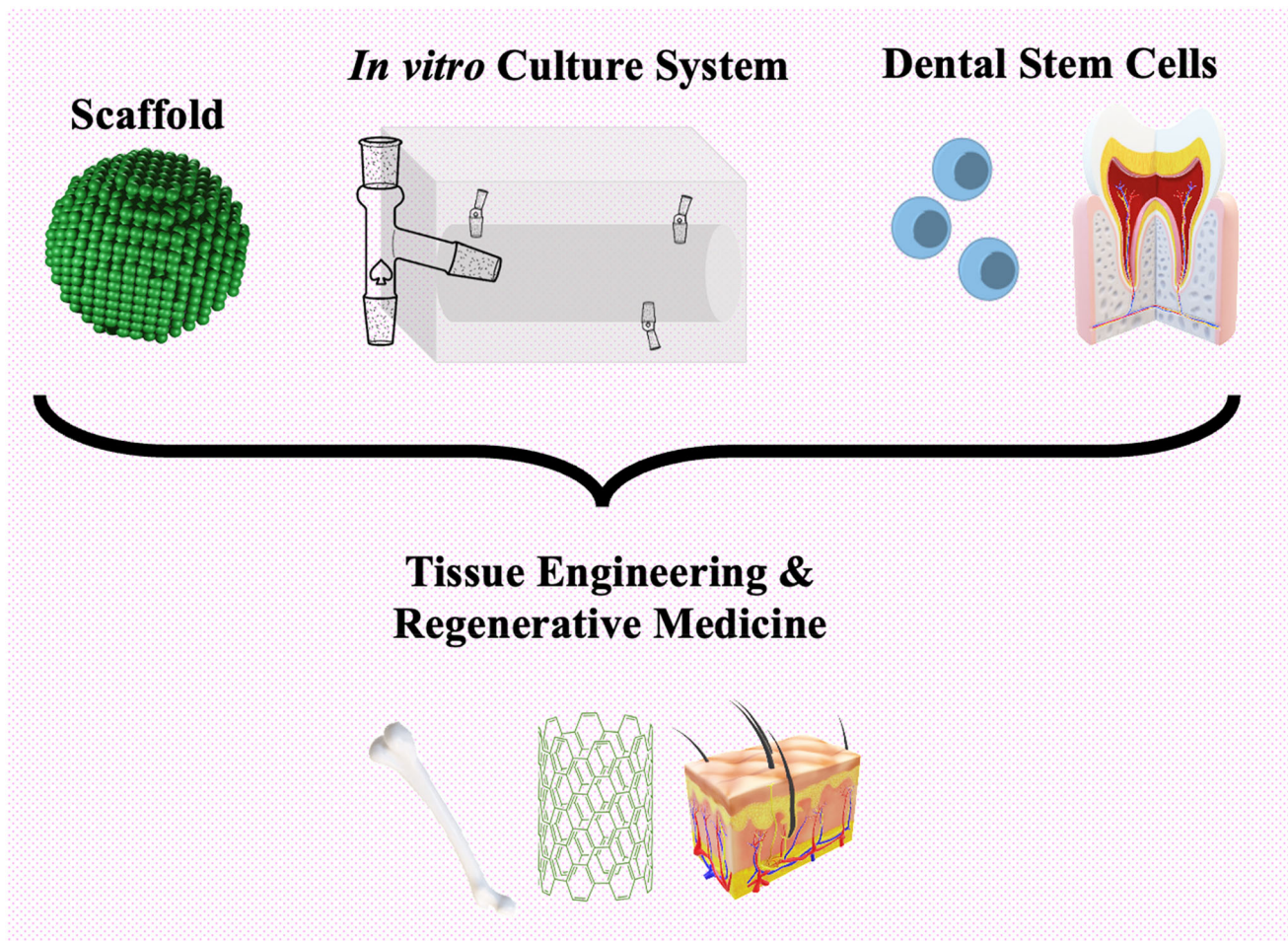


**Fig. 24** Dental stem cell-based tissue engineering. *in vitro* 3D tissue-engineered construct can be developed by combining dental stem cells with proper 3D cell carrier and bioreactor culture system, and can be applied to tissue engineering and regenerative medicine [142] Reconstructed from [Kim B-C, Bae H, Kwon I-K, Lee E-J, Park J-H,

Khademhosseini A, et al. Osteoblastic/cementoblastic and neural differentiation of dental stem cells and their applications to tissue engineering and regenerative medicine. *Tissue Eng Part B Rev.* 2012;18:235–44]

organization with intercalation of cells and NMs. Current findings reveal that periodontal tissues possess multi-potent (or dental) stem cells that have the potential for TE (Fig. 24) [142].

Xi et al. fabricated a biofilm using PCL-based vesicles, demonstrating good biocompatibility and antibacterial characteristics with a potential role in periodontitis therapy (Fig. 25A) [143]. Another strategy was proposed by Bao et al. as they have innovated a reactive oxygen species (ROS) scavenger using polydopamine in periodontal tissue. Their results demonstrate decreased inflammation and increased performance as ROS scavengers (Fig. 25B) [144]. A recent investigation conducted by Zhang et al., showed that they have innovated a bioscaffold using Au nanocages, which can be activated by light and possess antibacterial activity (Fig. 25C) [145].

#### 4.5 Skin tissue engineering applications

A substitute for the conventional wound healing approach is artificial skin regeneration. CP possesses antibacterial properties [20, 146, 147] and supports the growth of keratinocytes and fibroblasts [20, 148]. Different applications of NMs in skin TE are briefly discussed and summarized in Table 5.

Fabrication of conductive silicate hydrate (CSH) hydrogel in the presence of  $\text{FeCl}_3$ , by free radical polymerization of poly(acrylic acid) (PAA) and conductive, i.e., PPy on decorated chitosan (Dch-PPy), mimics human skin. The hydrogels have self-healing properties with 90% efficiency of electrical recovery in 2 min and 30 s, respectively. This is due to the dynamic ionic attraction of ferric ( $\text{Fe}^{3+}$ ) ions and the -NH functional groups of PPy with the carboxylic functional groups of PAA (Fig. 26). Ionic interactions among the functional groups of PAA and

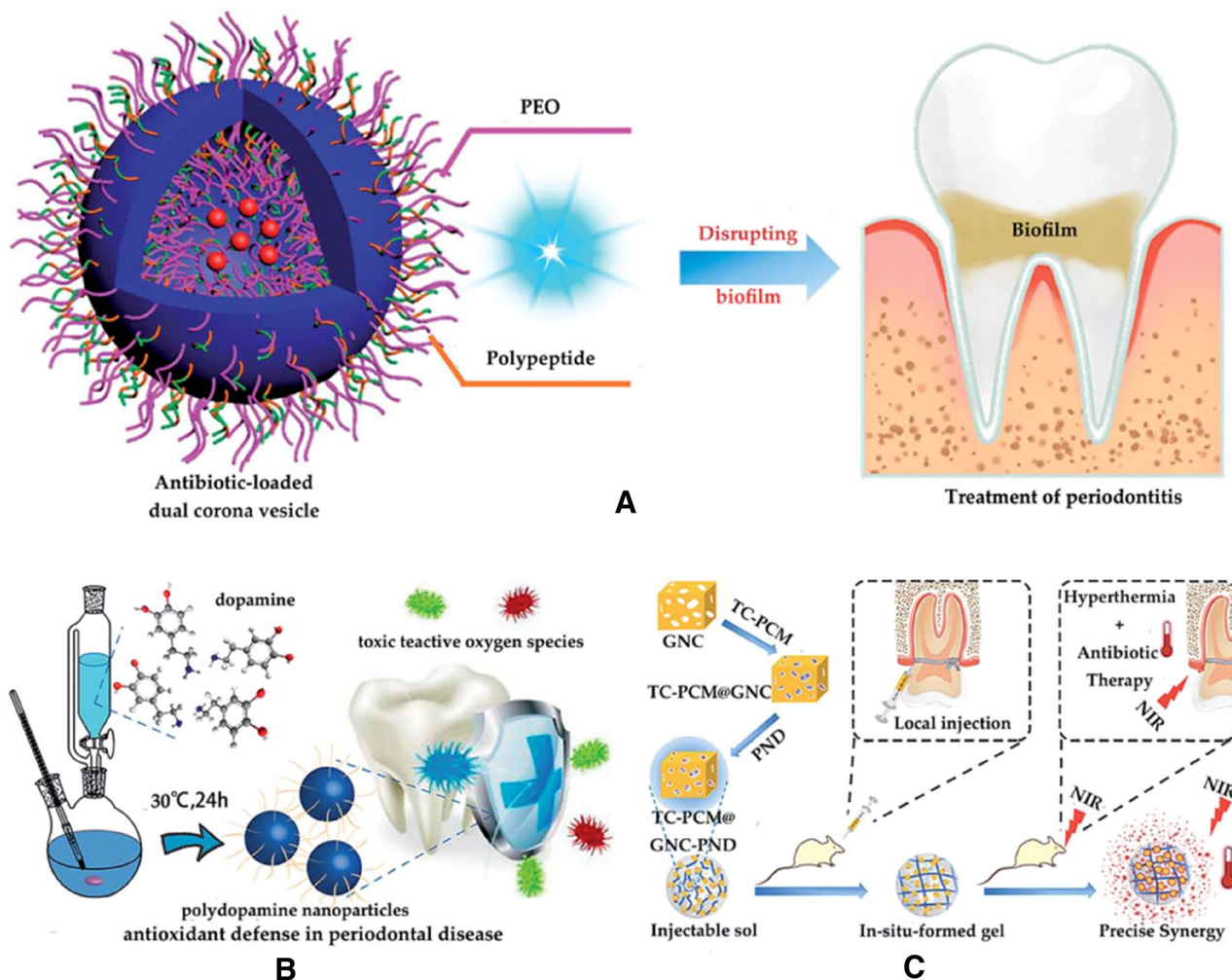


**Fig. 25** **A** Treatment of periodontitis with PCL-based vesicles. Reprinted with permission, [143] Copyright © 2019, American Chemical Society. **B** The synthesis of polydopamine nanomaterials and their usage as efficient reactive oxygen species scavengers in periodontitis. Reprinted with permission, [144] Copyright © 2018, American Chemical Society. **C** Schematic illustration of TC-

PCM@GNC-PND a combined platform for hyperthermia and antibiotics with an obvious synergistic antibacterial effect. *TC* Tetracycline, *PCM* phase-change materials, *GNC* Au nanocage, *PND* poly(N-isopropylacrylamide-co-diethylaminoethyl methylacrylate). Reprinted with permission, [145] Copyright © 2020, American Chemical Society

PPy may mediate self-healing, resulting in the migration of  $\text{Fe}^{3+}$  ions to the other side and the healing of the conductive self-healing hydrogel. Subsequently, the self-healing could be improved due to the H-bonding of PAA and CH. The mechanical strength of the conductive self-healing hydrogel was enhanced due to the covalent cross-linking between N, N'-methylenebis-acrylamide (MBAA) and PAA. The hydrogel also showed excellent performance in 3D printing, pressure sensitivity and stretchability [20, 55].

Another hydrogel fabricated by simply mixing CS-g-PA and PEG-co-poly(glycerol sebacate) (PGS) possesses biocompatible, antibacterial, electroactive, and free radical scavenger properties. Upregulation of GF expression for wound healing, full-thickness skin defect model, and showed good *in vivo* clotting and collagen deposition using

hydrogel. The hydrogel also exhibits tunable gelation time, adhesiveness, stiffness, conductivity, pore size, and swelling ratio by modulating crosslinking density [20, 86]. Lee et al. have fabricated a GO-poly(lactic-co-glycolic acid) (PLGA) composite with collagen (Col) hybrid fibre sheets via the dual electrospinning method and showed favorable results in wound healing implementation. They also showed increased proliferation of human dermal fibroblasts. The addition of GO enhanced the growth and differentiation of different SCs. Also, the presence of Col permits biochemical interaction with cells that mimics integrin-ECM attachment. The addition of GO and Col increased the hydrophilicity of fibre sheets while the decomposition temperature of fibre sheets was decreased by the addition of Col [50].

**Table 5** Skin tissue engineering applications

Nanocomposite	Synthesis method	Highlights	References
CSH/PAA/Dch-PPy	Free-radical polymerization	Mimic human skin	[20, 55]
CS-g-PA/PEG-co-PGS	The facile approach of mixing under physiological conditions	Antibacterial properties Wound healing <i>in vivo</i> clotting Collagen deposition	[20, 86]
GO-PLGA/Col hybrid fiber sheets	Dual electrospinning method	Wound healing Increased proliferation of human dermal fibroblasts (HDFs)	[50]
3D GF	CVD with Ni foam as a template	Wound healing Enhance growth and proliferation of MSCs Reduce scar formation Guides the wound healing process	[60]
HA-DA/rGO hydrogel dressing	EDC/NHS coupling	Wound healing Enhances vascularization Improve granulation tissue thickness Collagen deposition	[61]
GO-PEG/Que/Col scaffold	ECD-catalyzed amide formation under ultrasonication	Diabetic wound healing Promote collagen deposition Angiogenesis in diabetic wound repair Amplify attachment and proliferation of MSCs	[63]
MoSe <sub>2</sub> -NIPAM hydrogels	Simultaneous exfoliation and functionalization	Wound repair Tunable dual stimuli-responsive behavior	[57]
CS-Gel/nZnO scaffolds	In situ synthesis of nZnO NPs	Possess antibacterial and biodegradable properties	[56]

Rakhshaei et al. have fabricated a CS-gelatin (Gel) and nZnO composite hydrogel scaffold using in situ fabrication of ZnO NPs and thus enabled it to possess flexibility, antibacterial and drug delivery characteristics. Its compatibility was demonstrated by utilizing human dermal fibroblast cells (HFF2). The cells were attached to the hydrogel scaffold and they started to spread onto the hydrogel after incubation for 2 days. Moreover, the hydrogel showed an excellent swelling ratio, sustained biodegradation and a highly porosity nature that was useful in absorbing volumes of wound exudate [56]. Lei et al. demonstrated the potential use of a MoSe<sub>2</sub>-(poly (N-isopropylacrylamide-co-IL) (PNIL) hydrogel in wound repair and dual stimuli-responsive behavior by simultaneous exfoliation and functionalizing it. In hydrogels, N-isopropyl acrylamide (NIPAM) co-monomers have thermo-responsive characteristics. While MoSe<sub>2</sub> nanosheets act as photothermal means, they form a photo- and thermo-responsive hydrogel that can be administered remotely via laser exposure or non-exposure (Fig. 27). This dual nature was reversible and tunable by modulating the hydrophilic and hydrophobic properties of PNIL. The hydrogel was

highly stable in water due to the formation of a non-covalent bond among MoSe<sub>2</sub> nanosheets and PNIL through attachment with 1-vinylimidazole rings that form a crosslinking network [57].

Li et al. functionalized 3D graphene foam (GF) with BMSCs via the CVD method with Ni foams as a template and showed their potential to promote wound healing and also reduce scar generation owing to biochemical and biomechanical signals from GFs. The GFs have exceptional biocompatibility and enhance MSC growth and proliferation. Moreover, MSCs enhanced vascularization and laid out a healthier neo-skin. The only GFs that affected wound closure were GFs with MSCs that synergized to assist wound closure [60]. Chu et al. developed a PEGylated GO-modified quercetin-modified hybrid collagen scaffold using ECD-catalyzed amide formation under ultrasonication, and their results showed promising use in diabetic wound healing, promoting collagen deposition, and also amplifying attachment and proliferation of MSCs. Moreover, hydrogels showed excellent stability and adjustability of quercetin conduction capacity for stimulating MSCs' differentiation into adipocyte and osteoblast,

**Fig. 26** Schematically depicted the mechanism of self-healing after a cut that is mediated by conductive self-healing hydrogels. Reprinted with permission, [55] Copyrights © 2016 WILEY-VCH Verlag GmbH & Co. KGaA, Weinheim

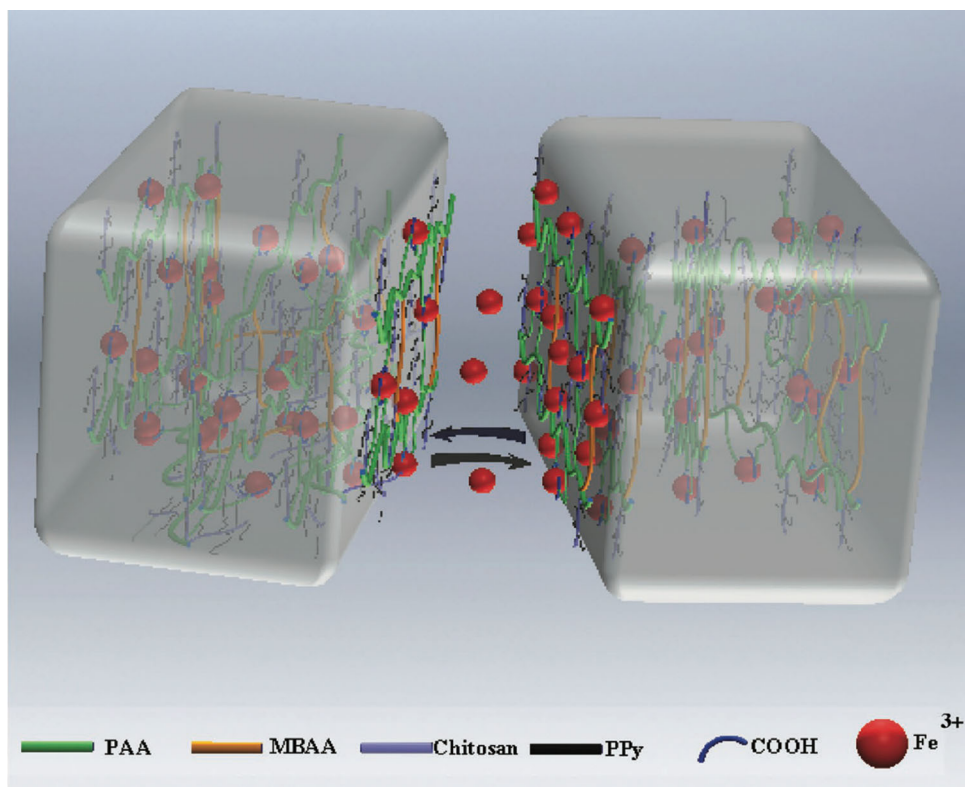
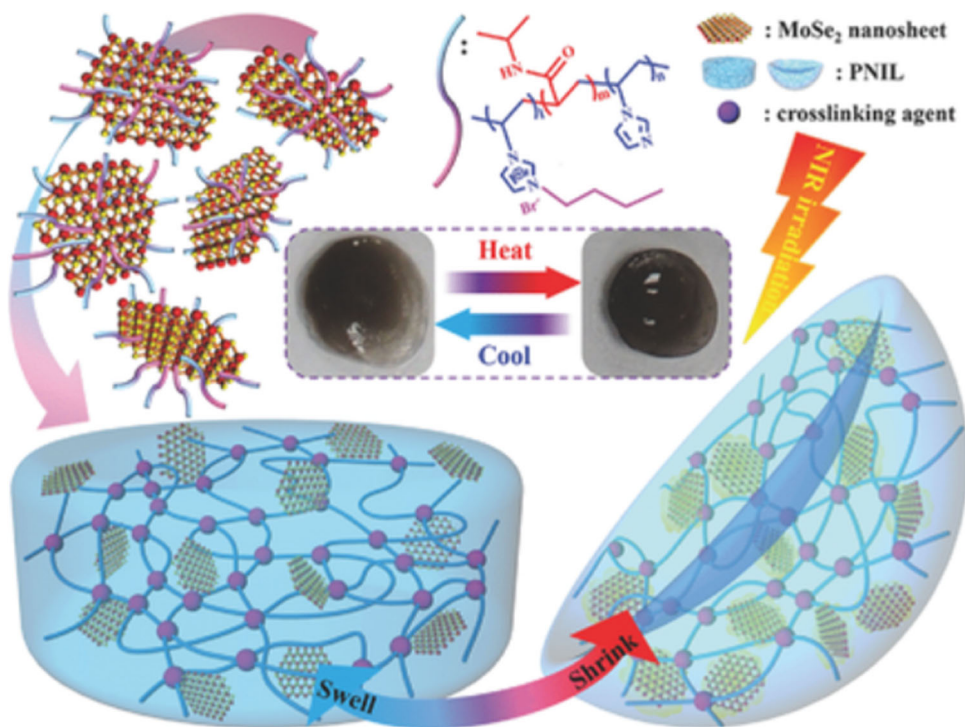


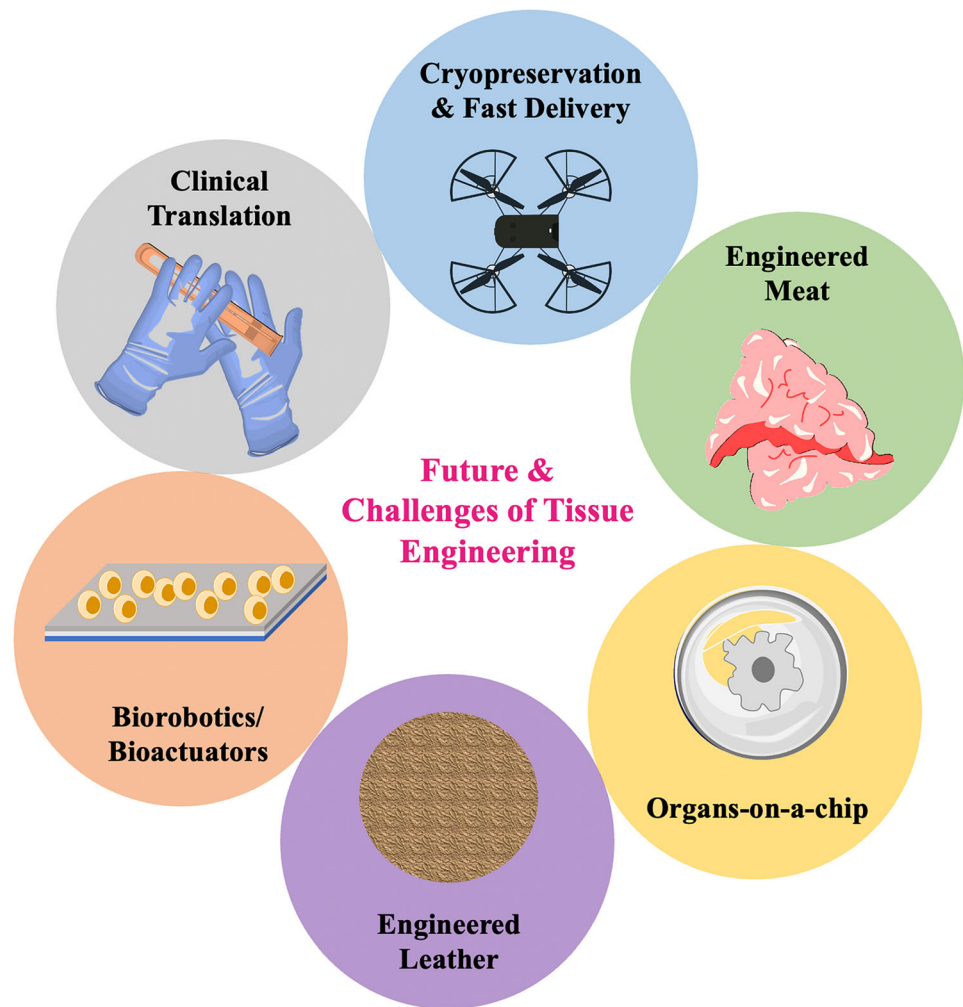
**Fig. 27** Schematic representation of reversible swelling or shrinking motions of the hydrogels with cooling or heating stimulations. A PNIL assisted non-covalent assembly of functionalized MoS<sub>2</sub> nanosheets to form a novel nanocomposite that exhibit dual behavior, i.e., photo- and thermo-responsive nature and results in shrinking or swelling. Reprinted with permission, [57] Copyrights © 2016 WILEY-VCH Verlag GmbH & Co. KGaA, Weinheim



a biodegradable nanofiber interface, and controllable drug release capability *in vitro*. In wound healing process, the wound closure percentage treated with scaffolds showed a faster gradual rate after 7 days of incubation of scaffolds.

After 14 days, hair follicles and mature vessels were realized in dermis. No fur appeared and hypertrophic scarring occurred around the diabetic wound after 21 days [63].

**Fig. 28** Future and challenges of tissue engineering: clinical translation, organ-on-a-chip and disease modelling, biorobotics, engineered meat and leather, cryopreservation and fast delivery [6] (Reconstructed from [Khademhosseini A, Langer RA. decade of progress in tissue engineering. Nat Protoc. 2016;11:1775–81])



Liang et al. fabricated a HA-graft-DA with rGO (HA-DA/rGO) hydrogel dressing via oxidative coupling of EDC/NHS and their results showed enhanced vascularization, improved granulation tissue thickness, collagen deposition, and their potential use in wound healing applications. The hydrogels generated thicker granulation tissue than Tegaderm films after 14 days of incubation, which led to excellent wound healing effects. The hydrogels also revealed high swelling, tunable rheological properties, degradability, and excellent mechanical features for human skin [61].

## 5 Challenges and future perspectives

Despite many advancements, further innovation is required to encounter many obstacles in the translation of theoretical aspects into reality. One of the demerits is the inefficacy of engineered biological mimics to substitute for characteristics exhibited by natural tissues [1]. Their ability to

perform cellular functions and the accumulation of NPs over time are major shortcomings that still need to be looked into. Another important aspect is the accumulation of the functionalized polymer over time. To overcome this paradigm, scientists have adopted several strategies to fabricate varied compositions of polymers for their possible application in clinical and biological settings. Biodegradable polymers have grasped recent consideration due to numerous characteristics such as structural precision, porosity, degradation and many more [19]. Also, the verification or validation of *in vitro* studies using *in vivo* experiments is scarce today and is crucial for their accomplished use in biomedicine. Many applications already exist in the literature, reinforcing the application of NMs as a potential candidate for TE-associated strategies and also with the involvement of stem cell-directed proliferation and regeneration of tissues as a promising future.

A lot of research in TE has focused on experiments using animals as models and is therefore inadequate for implementation in human systems. Also, to achieve

efficient NM-enabled biological tissue, factors such as prolonged safety, toxicity, biodegradability and biocompatibility in the living system need to be considered thoroughly along with systemic research [4]. Furthermore, certain future prospects and demerits that include organ-on-a-chip, biorobotics, clinical translation and many more have been illustrated (Fig. 28) [6].

A major challenge associated with techniques ranging from electrospinning to injection molding is the fabrication of scaffolds with optimized porosity, morphology and interconnectivity. To circumvent this, DIW [37] and 3D printing [15] (in peculiar) are being employed because of their effectiveness [14, 38].

For applications in biomedical fields, the development of a suitable composite hydrogel is crucial, which depends on the conductive material along with suitable blending strategies and manufacturing strategies [20]. Appropriate use of NM with polymers has the potential to improve electrical, mechanical and biological properties significantly. Therefore, it could serve a diversity of functions as per the applications. In addition to the aforementioned properties, several NMs functionalized biocomposite scaffolds have been shown to possess antibacterial properties and thus could protect the reconstructive tissue against infection, sepsis and implant malfunctioning [1].

## 6 Conclusion

As of now, the use of NMs in TE is scarce. However, recent literature suggests significant potential for medical use, such as directed stem cell proliferation and differentiation, the formation of tissue and organs, implantation, and regenerative roles. The present review summarizes current advancements in NPs that have speedily come to the forefield of TE and their successful application in cardiac, neural, bone, dental and skin tissues. Before highlighting the aforementioned applications, we have explored the generic fabrication methods for synthesizing bioscaffolds and conductive hydrogels possessing the ability to mimic the ECM using methods such as 3D printing and DIW, which have grabbed immense attention recently because of their effectiveness and design flexibility. We have tabulated several nanocomposites and highlighted their usage in different bioengineering areas. With the invention of new approaches, certain challenges remain to be dealt with for their propitious use in future methodology and we have talked through a few of them, followed by future perspectives. Furthermore, we have accentuated the potential use of NPs for associated methodologies. Along with their optimistic association with directed stem cell proliferation and regenerative medicine.

**Acknowledgement** The author SK and Bhawna thanks for Senior Research Fellowship from Council of Scientific & Industrial Research (File No. 08/694(0004)/2018-EMR-I) and University Grant Commission, respectively.

## Declarations

**Conflict of interest** Prashant Singh, Vinod Kumar and Akanksha Gupta (the Corresponding Authors) declare that this manuscript is original, has not been published before and is not currently being considered for publication elsewhere. We further confirm that the order of authors listed in the manuscript has been approved by all of us. The authors also declare that they have no known competing financial interests or personal relationships that could have appeared to influence the work reported in this paper.

**Research involving human participants and/or animals** It is declared that no human participants and/or animals are used in this work. It is a review article.

## References

- Hasan A, Morshed M, Memic A, Hassan S, Webster TJ, Marei HE. Nanoparticles in tissue engineering: applications, challenges and prospects. *Int J Nanomedicine*. 2018;13:5637.
- Paul A, Manoharan V, Krafft D, Assmann A, Uquillas JA, Shin SR, et al. Nanoengineered biomimetic hydrogels for guiding human stem cell osteogenesis in three dimensional microenvironments. *J Mater Chem B*. 2016;4:3544–54.
- Hasan A, Paul A, Memic A, Khademhosseini AA. multilayered microfluidic blood vessel-like structure. *Biomed Microdev*. 2015;17:1–13.
- Zhang J, Chen H, Zhao M, Liu G, Wu J. 2D nanomaterials for tissue engineering application. *Nano Res*. 2020;13:2019–34.
- Zheng X, Zhang P, Fu Z, Meng S, Dai L, Yang H. Applications of nanomaterials in tissue engineering. *RSC Adv*. 2021;11:19041–58.
- Khademhosseini A, Langer RA. decade of progress in tissue engineering. *Nat Protoc*. 2016;11:1775–81.
- Opris I, Lebedev MA, Pulgar VM, Vidu R, Enachescu M, Casanova MF. Nanotechnologies in neuroscience and neuro-engineering. *Front Neurosci*. 2020;14:33.
- Tu Z, Guday G, Adeli M. and Haag R Multivalent interactions between 2D nanomaterials and biointerfaces. *Adv Mater*. 2018;30:1706709.
- Huang K, Wu J, Gu Z. Black phosphorus hydrogel scaffolds enhance bone regeneration via a sustained supply of calcium-free phosphorus. *ACS Appl Mater Interfaces*. 2018;11:2908–16.
- Wang S, Shao J, Li Z, Ren Q, Yu XF, Liu S. Black phosphorus-based multimodal nanoagent: Showing targeted combinatory therapeutics against cancer metastasis. *Nano Lett*. 2019;19:5587–94.
- Luo M, Fan T, Zhou Y, Zhang H, Mei L. 2D black phosphorus-based biomedical applications. *Adv Funct Mater*. 2019;29:1808306.
- Liu Z, Chen H, Jia Y, Zhang W, Zhao H, Fan W, et al. A two-dimensional fingerprint nanoprobe based on black phosphorus for bio-SERS analysis and chemo-photothermal therapy. *Nanoscale*. 2018;10:18795–804.
- Kurapati R, Kostarelos K, Prato M, Bianco A. Biomedical uses for 2D materials beyond graphene: current advances and challenges ahead. *Adv Mater*. 2016;28:6052–74.
- Mohan T, Dobaj Štiglic A, Beaumont M, Konnerth J, Gürer F, Makuc D, et al. Generic method for designing self-standing and

- dual porous 3D bioscaffolds from cellulosic nanomaterials for tissue engineering applications. *ACS Appl Bio Mater.* 2020;3:1197–209.
15. Mohan T, Maver T, Štiglic AD, Stana-Kleinschek K, Kargl R. 3D bioprinting of polysaccharides and their derivatives: from characterization to application. In: *Fundamental biomaterials: polymers.* Elsevier; 2018. p. 105–41.
  16. Asadi N, Del Bakhshayesh AR, Davaran S, Akbarzadeh A. Common biocompatible polymeric materials for tissue engineering and regenerative medicine. *Mater Chem Phys.* 2020;242:122528.
  17. Rahmati M, Pennisi CP, Budd E, Mobasheri A, Mozafari M. Biomaterials for regenerative medicine: historical perspectives and current trends. In: *Cell biology and translational medicine, vol. 4.* Springer; 2018. p. 1–19.
  18. Rahmani Del Bakhshayesh A, Annabi N, Khalilov R, Akbarzadeh A, Samiei M, Alizadeh E, et al. Recent advances on biomedical applications of scaffolds in wound healing and dermal tissue engineering. *Artif Cells Nanomed Biotechnol.* 2018;46:691–705.
  19. Iqbal N, Khan AS, Asif A, Yar M, Haycock JW, Rehman IU. Recent concepts in biodegradable polymers for tissue engineering paradigms: a critical review. *Int Mater Rev.* 2019;64:91–126.
  20. Min JH, Patel M, Koh WG. Incorporation of conductive materials into hydrogels for tissue engineering applications. *Polymers.* 2018;10:1078.
  21. Souier T, Stefancich M, Chiesa M. Characterization of multi-walled carbon nanotube–polymer nanocomposites by scanning spreading resistance microscopy. *Nanotechnology.* 2012;23:405704.
  22. Patton AJ, Poole-Warren LA, Green RA. Mechanisms for imparting conductivity to nonconductive polymeric biomaterials. *Macromol Biosci.* 2016;16:1103–21.
  23. Gaharwar AK, Peppas NA, Khademhosseini A. Nanocomposite hydrogels for biomedical applications. *Biotechnol Bioeng.* 2014;111:441–53.
  24. Kaur G, Adhikari R, Cass P, Bown M, Gunatillake P. Electrically conductive polymers and composites for biomedical applications. *RSC Adv.* 2015;5:37553–67.
  25. Shevach M, Fleischer S, Shapira A, Dvir T. Gold nanoparticle-decellularized matrix hybrids for cardiac tissue engineering. *Nano Lett.* 2014;14:5792–6.
  26. Guo B, Ma PX. Conducting polymers for tissue engineering. *Biomacromol.* 2018;19:1764–82.
  27. Powar PV. Development status in the meadow of nanostructure magnetic drug delivery system and its promising applications. *Int J Pharm Pharm Sci.* 2017;9:10–7.
  28. Doberenz F, Zeng K, Willems C, Zhang K, Groth T. Thermoresponsive polymers and their biomedical application in tissue engineering—a review. *J Mater Chem B.* 2020;8:607–28.
  29. Menon MP, Selvakumar R, Ramakrishna S. Extraction and modification of cellulose nanofibers derived from biomass for environmental application. *RSC Adv.* 2017;7:42750–73.
  30. Apelgren P, Karabulut E, Amoroso M, Mantas A, Hc MÁ, Kölby L, et al. In vivo human cartilage formation in three-dimensional bioprinted constructs with a novel bacterial nanocellulose bioink. *ACS Biomater Sci Eng.* 2019;5:2482–90.
  31. Nguyen D, Hägg DA, Forsman A, Ekholm J, Nimkingratana P, Brantsing C, et al. Cartilage tissue engineering by the 3D bioprinting of iPS cells in a nanocellulose/alginate bioink. *Sci Rep.* 2017;7:658.
  32. Nasri-Nasrabadi B, Mehrasa M, Rafienia M, Bonakdar S, Behzad T, Gavanji S. Porous starch/cellulose nanofibers composite prepared by salt leaching technique for tissue engineering. *Carbohydr Polym.* 2014;108:232–8.
  33. Zhang J, Chang P, Zhang C, Xiong G, Luo H, Zhu Y, et al. Immobilization of lecithin on bacterial cellulose nanofibers for improved biological functions. *React Funct Polym.* 2015;91:100–7.
  34. Maver T, Smrke D, Kurečič M, Gradišnik L, Maver U, Kleinschek KS. Combining 3D printing and electrospinning for preparation of pain-relieving wound-dressing materials. *J Solgel Sci Technol.* 2018;88:33–48.
  35. Petta D, Armiento A, Grijpma D, Alini M, Eglin D, D'Este M. 3D bioprinting of a hyaluronan bioink through enzymatic-and visible light-crosslinking. *Biofabrication.* 2018;10:044104.
  36. Sampath UG, Ching YC, Chuah CH, Sabariah JJ, Lin PC. Fabrication of porous materials from natural/synthetic biopolymers and their composites. *Mater.* 2016;9:991.
  37. Cidonio G, Glinka M, Dawson J, Oreffo R. The cell in the ink: Improving biofabrication by printing stem cells for skeletal regenerative medicine. *Biomaterials.* 2019;209:10–24.
  38. Wang X, Lou T, Zhao W, Song G, Li C, Cui G. The effect of fiber size and pore size on cell proliferation and infiltration in PLLA scaffolds on bone tissue engineering. *J Biomater Appl.* 2016;30:1545–51.
  39. Saravanan S, Sareen N, Abu-El-Rub E, Ashour H, Sequiera GL, Ammar HI, et al. Graphene oxide-gold nanosheets containing chitosan scaffold improves ventricular contractility and function after implantation into infarcted heart. *Sci Rep.* 2018;8:15069.
  40. Kaur T, Thirugnanam A. Tailoring in vitro biological and mechanical properties of polyvinyl alcohol reinforced with threshold carbon nanotube concentration for improved cellular response. *RSC Adv.* 2016;6:39982–92.
  41. Wang H, Han H, Ma Z. Conductive hydrogel composed of 1, 3, 5-benzenetricarboxylic acid and Fe<sup>3+</sup> used as enhanced electrochemical immunosensing substrate for tumor biomarker. *Bioelectrochemistry.* 2017;114:48–53.
  42. Heo DN, Ko WK, Bae MS, Lee JB, Lee DW, Byun W, et al. Enhanced bone regeneration with a gold nanoparticle–hydrogel complex. *J Mater Chem B.* 2014;2:1584–93.
  43. Chahal S, Hussain FSJ, Yusoff MBM. Characterization of modified cellulose (MC)/poly (vinyl alcohol) electrospun nanofibers for bone tissue engineering. *Procedia Eng.* 2013;53:683–8.
  44. Nazari H, Heirani-Tabasi A, Hajiabbas M, Khalili M, Shahsavari Alavijeh M, Hatamie S, et al. Incorporation of two-dimensional nanomaterials into silk fibroin nanofibers for cardiac tissue engineering. *Polym Adv Technol.* 2020;31:248–59.
  45. Liang Y, Mitriashkin A, Lim TT, Goh JC. Conductive polypyrrole-encapsulated silk fibroin fibers for cardiac tissue engineering. *Biomaterials.* 2021;276:121008.
  46. Honkamäki L, Joki T, Grigoryev NA, Levon K, Ylä-Outinen L, Narkilahti S. Novel method to produce a layered 3D scaffold for human pluripotent stem cell-derived neuronal cells. *J Neurosci Methods.* 2021;350:109043.
  47. Mahmoudi N, Simchi A. On the biological performance of graphene oxide-modified chitosan/polyvinyl pyrrolidone nanocomposite membranes: in vitro and in vivo effects of graphene oxide. *Mater Sci Eng C Mater Biol Appl.* 2017;70:121–31.
  48. Unnithan AR, Sasikala ARK, Park CH, Kim CSA. unique scaffold for bone tissue engineering: an osteogenic combination of graphene oxide–hyaluronic acid–chitosan with simvastatin. *J Ind Eng Chem.* 2017;46:182–91.
  49. Rodrigues BV, Silva AS, Melo GF, Vasconcellos LM, Marciano FR, Lobo AO. Influence of low contents of superhydrophilic MWCNT on the properties and cell viability of electrospun poly (butylene adipate-co-terephthalate) fibers. *Mater Sci Eng C Mater Biol Appl.* 2016;59:782–91.

50. Lee EJ, Lee JH, Shin YC, Hwang DG, Kim JS, Jin OS, et al. Graphene oxide-decorated PLGA/collagen hybrid fiber sheets for application to tissue engineering scaffolds. *Biomater Res*. 2014;18:18–24.
51. Yang J, Wang X, Wang X, Jia R, Huang J. Preparation of highly conductive CNTs/polyaniline composites through plasma pre-treating and in-situ polymerization. *J Phys Chem Solids*. 2010;71:448–52.
52. Kim YS, Cho K, Lee HJ, Chang S, Lee H, Kim JH, et al. Highly conductive and hydrated PEG-based hydrogels for the potential application of a tissue engineering scaffold. *React Funct Polym*. 2016;109:15–22.
53. Luo X, Cui XT. Sponge-like nanostructured conducting polymers for electrically controlled drug release. *Electrochem Commun*. 2009;11:1956–9.
54. Shi Z, Gao H, Feng J, Ding B, Cao X, Kuga S, et al. In situ synthesis of robust conductive cellulose/polypyrrole composite aerogels and their potential application in nerve regeneration. *Angew Chem Int Ed*. 2014;53:5380–4.
55. Darabi MA, Khosrozadeh A, Mbeleck R, Liu Y, Chang Q, Jiang J, et al. Skin-inspired multifunctional autonomic-intrinsic conductive self-healing hydrogels with pressure sensitivity, stretchability, and 3D printability. *Adv Mater*. 2017;29:1700533.
56. Rakhshaei R, Namazi H, Hamishehkar H, Kafil HS, Salehi R. In situ synthesized chitosan–gelatin/ZnO nanocomposite scaffold with drug delivery properties: Higher antibacterial and lower cytotoxicity effects. *J Appl Polym Sci*. 2019;136:47590.
57. Lei Z, Zhou Y, Wu P. Simultaneous exfoliation and functionalization of MoSe<sub>2</sub> nanosheets to prepare “smart” nanocomposite hydrogels with tunable dual stimuli-responsive behavior. *Small*. 2016;12:3112–8.
58. Gupta ND, Maity S, Chattopadhyay KK. Field emission enhancement of polypyrrole due to band bending induced tunnelling in polypyrrole-carbon nanotubes nanocomposite. *J Ind Eng Chem*. 2014;20:3208–13.
59. Li H, Zhao Q, Li B, Kang J, Yu Z, Li Y, et al. Fabrication and properties of carbon nanotube-reinforced hydroxyapatite composites by a double in situ synthesis process. *Carbon*. 2016;101:159–67.
60. Li Z, Wang H, Yang B, Sun Y, Huo R. Three-dimensional graphene foams loaded with bone marrow derived mesenchymal stem cells promote skin wound healing with reduced scarring. *Mater Sci Eng C Mater Biol Appl*. 2015;57:181–8.
61. Liang Y, Zhao X, Hu T, Chen B, Yin Z, Ma PX, et al. Adhesive hemostatic conducting injectable composite hydrogels with sustained drug release and photothermal antibacterial activity to promote full-thickness skin regeneration during wound healing. *Small*. 2019;15:1900046.
62. Paul A, Hasan A, Kindi HA, Gaharwar AK, Rao VT, Nikkha M, et al. Injectable graphene oxide/hydrogel-based angiogenic gene delivery system for vasculogenesis and cardiac repair. *ACS Nano*. 2014;8:8050–62.
63. Chu J, Shi P, Yan W, Fu J, Yang Z, He C, et al. PEGylated graphene oxide-mediated quercetin-modified collagen hybrid scaffold for enhancement of MSCs differentiation potential and diabetic wound healing. *Nanoscale*. 2018;10:9547–60.
64. Deliormanlı AM. Direct write assembly of graphene/poly ( $\epsilon$ -caprolactone) composite scaffolds and evaluation of their biological performance using mouse bone marrow mesenchymal stem cells. *Appl Biochem Biotechnol*. 2019;188:1117–33.
65. Jing X, Mi HY, Napiwocki BN, Peng XF, Turng LS. Mussel-inspired electroactive chitosan/graphene oxide composite hydrogel with rapid self-healing and recovery behavior for tissue engineering. *Carbon*. 2017;125:557–70.
66. Liu N, Chen J, Zhuang J, Zhu P. Fabrication of engineered nanoparticles on biological macromolecular (PEGylated chitosan) composite for bio-active hydrogel system in cardiac repair applications. *Int J Biol Macromol*. 2018;117:553–8.
67. Choe G, Kim SW, Park J, Park J, Kim S, Kim YS, et al. Antioxidant activity reinforced reduced graphene oxide/alginate microgels: mesenchymal stem cell encapsulation and regeneration of infarcted hearts. *Biomaterials*. 2019;225:119513.
68. Xu C, Wu F, Yu P, Mao L. In vivo electrochemical sensors for neurochemicals: recent update. *ACS Sens*. 2019;4:3102–18.
69. Kim Y, Meade SM, Chen K, Feng H, Rayyan J, Hess-Dunning A, et al. Nano-architectural approaches for improved intracortical interface technologies. *Front Neurosci*. 2018;12:456.
70. Samadian H, Ehterami A, Sarrafzadeh A, Khashtar H, Nikbakht M, Rezaei A, et al. Sophisticated polycaprolactone/gelatin nanofibrous nerve guided conduit containing platelet-rich plasma and citicoline for peripheral nerve regeneration: in vitro and in vivo study. *Int J Biol Macromol*. 2020;150:380–8.
71. Schulte C, Lamanna J, Moro AS, Piazzoni C, Borghi F, Chighizola M, et al. Neuronal cells confinement by micropatterned cluster-assembled dots with mechanotransductive nanotopography. *ACS Biomater Sci Eng*. 2018;4:4062–75.
72. Ryyänen T, Toivanen M, Salminen T, Ylä-Outinen L, Narkilahti S, Lekkala J. Ion beam assisted E-beam deposited TiN microelectrodes—applied to neuronal cell culture medium evaluation. *Front Neurosci*. 2018;12:882.
73. Satir TM, Nazir FH, Vizlin-Hodzic D, Hardselius E, Blennow K, Wray S, et al. Accelerated neuronal and synaptic maturation by BrainPhys medium increases A $\beta$  secretion and alters A $\beta$  peptide ratios from iPSC-derived cortical neurons. *Sci Rep*. 2020;10:601.
74. Shih M, Kuo CT, Lin MH, Chuang YJ, Chen H, Yew TR. 3D-CNT micro-electrode array for zebrafish ECG study including directionality measurement and drug test. *Biocybern Biomed Eng*. 2020;40:701–8.
75. Pelkonen A, Mzezewa R, Sukki L, Ryyänen T, Kreutzer J, Hyvärinen T, et al. A modular brain-on-a-chip for modelling epileptic seizures with functionally connected human neuronal networks. *Biosens Bioelectron*. 2020;168:112553.
76. Kumar R, Aadil KR, Ranjan S, Kumar VB. Advances in nanotechnology and nanomaterials based strategies for neural tissue engineering. *J Drug Deliv Sci Technol*. 2020;57:101617.
77. Jin G-Z, Kim M, Shin US, Kim HW. Neurite outgrowth of dorsal root ganglia neurons is enhanced on aligned nanofibrous biopolymer scaffold with carbon nanotube coating. *Neurosci Lett*. 2011;501:10–4.
78. Miao Y, Shi X, Li Q, Hao L, Liu L, Liu X, et al. Engineering natural matrices with black phosphorus nanosheets to generate multi-functional therapeutic nanocomposite hydrogels. *Biomater Sci*. 2019;7:4046–59.
79. Liu X, Miller AL, Park S, George MN, Waletzki BE, Xu H, et al. Two-dimensional black phosphorus and graphene oxide nanosheets synergistically enhance cell proliferation and osteogenesis on 3D printed scaffolds. *ACS Appl Mater Interfaces*. 2019;11:23558–72.
80. Ghaderinejad P, Najmoddin N, Bagher Z, Saeed M, Karimi S, Simorgh S, et al. An injectable anisotropic alginate hydrogel containing oriented fibers for nerve tissue engineering. *Chem Eng J*. 2021;420:130465.
81. Diez-Pascual AM, Diez-Vicente AL. Poly (propylene fumarate)/polyethylene glycol-modified graphene oxide nanocomposites for tissue engineering. *ACS Appl Mater Interfaces*. 2016;8:17902–14.
82. Zhao Y, Chen J, Zou L, Xu G, Geng Y. Facile one-step bioinspired mineralization by chitosan functionalized with graphene



- oxide to activate bone endogenous regeneration. *Chem Eng J*. 2019;378:122174.
83. Pahlevanzadeh F, Bakhsheshi-Rad H, Hamzah E. In-vitro biocompatibility, bioactivity, and mechanical strength of PMMA-PCL polymer containing fluorapatite and graphene oxide bone cements. *J Mech Behav Biomed Mater*. 2018;82:257–67.
  84. Miyaji H, Murakami S, Nishida E, Akasaka T, Fugetsu B, Umeda J, et al. Evaluation of tissue behavior on three-dimensional collagen scaffold coated with carbon nanotubes and  $\beta$ -tricalcium phosphate nanoparticles. *J Tissue Eng*. 2018;15:123–30.
  85. Chen WY, Yang RC, Wang HM, Zhang L, Hu K, Li CH, et al. Self-assembled heterojunction carbon nanotubes synergizing with photoimmobilized IGF-1 inhibit cellular senescence. *Adv Healthc Mater*. 2016;5:2413–26.
  86. Zhao X, Wu H, Guo B, Dong R, Qiu Y, Ma PX. Antibacterial anti-oxidant electroactive injectable hydrogel as self-healing wound dressing with hemostasis and adhesiveness for cutaneous wound healing. *Biomaterials*. 2017;122:34–47.
  87. Bohner M, Loosli Y, Baroud G, Lacroix D. Commentary: deciphering the link between architecture and biological response of a bone graft substitute. *Acta Biomater*. 2011;7:478–84.
  88. Jung CS, Kim BK, Lee J, Min BH, Park SH. Development of printable natural cartilage matrix bioink for 3D printing of irregular tissue shape. *Tissue Eng Regen Med*. 2018;15:155–62.
  89. Markstedt K, Mantas A, Tournier I, Martínez Ávila H, Hagg D, Gatenholm P. 3D bioprinting human chondrocytes with nanocellulose–alginate bioink for cartilage tissue engineering applications. *Biomacromol*. 2015;16:1489–96.
  90. Huan S, Ajdary R, Bai L, Klar V, Rojas OJ. Low solids emulsion gels based on nanocellulose for 3D-printing. *Biomacromol*. 2018;20:635–44.
  91. Tchobanian A, Van Oosterwyck H, Fardim P. Polysaccharides for tissue engineering: current landscape and future prospects. *Carbohydr Polym*. 2019;205:601–25.
  92. Xue J, Wu T, Dai Y, Xia YJ. Electrospinning and electrospun nanofibers: Methods, materials, and applications. *Chem Rev*. 2019;119:5298–415.
  93. Ardekani SR, Aghdam ASR, Nazari M, Bayat A, Yazdani E, Saievar-Iranizad E, et al. A comprehensive review on ultrasonic spray pyrolysis technique: Mechanism, main parameters and applications in condensed matter. *J Anal Appl Pyrolysis*. 2019;141:104631.
  94. Fu H, Xu H, Liu Y, Yang Z, Kormakov S, Wu D, et al. Overview of injection molding technology for processing polymers and their composites. *ES Mater Manuf*. 2020;8:3–23.
  95. Deb P, Deoghare AB, Borah A, Barua E, Lala SD. Scaffold development using biomaterials: a review. *Mater Today*. 2018;5:12909–19.
  96. Heid S, Boccaccini AR. Advancing bioinks for 3D bioprinting using reactive fillers: A review. *Acta Biomater*. 2020;113:1–22.
  97. Sinha SK. Additive manufacturing (AM) of medical devices and scaffolds for tissue engineering based on 3D and 4D printing. In: 3D and 4D printing of polymer nanocomposite materials. Elsevier; 2020. p. 119–60.
  98. Tamay DG, Dursun Usal T, Alagoz AS, Yucler D, Hasirci N, Hasirci V. 3D and 4D printing of polymers for tissue engineering applications. *Front Bioeng Biotechnol*. 2019;7:164.
  99. Mandrycky C, Wang Z, Kim K, Kim DH. 3D bioprinting for engineering complex tissues. *Biotechnol Adv*. 2016;34:422–34.
  100. Lai J, Zhang L, Niu W, Qi W, Zhao J, Liu Z, et al. One-pot synthesis of gold nanorods using binary surfactant systems with improved monodispersity, dimensional tunability and plasmon resonance scattering properties. *Nanotechnology*. 2014;25:125601.
  101. Dang ZM, Yuan JK, Zha JW, Zhou T, Li ST, Hu GH. Fundamentals, processes and applications of high-permittivity polymer–matrix composites. *Prog Mater Sci*. 2012;57:660–723.
  102. Kurniawan D, Nor F, Lee H, Lim J. Elastic properties of polycaprolactone at small strains are significantly affected by strain rate and temperature. *Proc Inst Mech Eng H*. 2011;225:1015–20.
  103. Ashtari K, Nazari H, Ko H, Tebon P, Akhshik M, Akbari M, et al. Electrically conductive nanomaterials for cardiac tissue engineering. *Adv Drug Deliv Rev*. 2019;144:162–79.
  104. Wei K, Serpooshan V, Hurtado C, Diez-Cunado M, Zhao M, Maruyama S, et al. Epicardial FSTL1 reconstitution regenerates the adult mammalian heart. *Nature*. 2015;525:479–85.
  105. Serpooshan V, Chen P, Wu H, Lee S, Sharma A, Hu DA, et al. Bioacoustic-enabled patterning of human iPSC-derived cardiomyocytes into 3D cardiac tissue. *Biomaterials*. 2017;131:47–57.
  106. Gálvez-Montón C, Prat-Vidal C, Roura S, Soler-Botija C, Bayes-Genis A. Cardiac tissue engineering and the bioartificial heart. *Revista Española de Cardiología (English Edition)*. 2013;66:391–9.
  107. Tomov ML, Gil CJ, Cetnar A, Theus AS, Lima BJ, Nish JE, et al. Engineering functional cardiac tissues for regenerative medicine applications. *Curr Cardiol Rep*. 2019;21:105.
  108. Lee J, Manoharan V, Cheung L, Lee S, Cha B-H, Newman P, et al. Nanoparticle-based hybrid scaffolds for deciphering the role of multimodal cues in cardiac tissue engineering. *ACS Nano*. 2019;13:12525–39.
  109. Choi YJ, Yi HG, Kim SW, Cho DW. 3D cell printed tissue analogues: a new platform for theranostics. *Theranostics*. 2017;7:3118–37.
  110. Pati F, Jang J, Ha DH, Kim SW, Rhie JW, Shim JH, et al. Printing three-dimensional tissue analogues with decellularized extracellular matrix bioink. *Nat Commun*. 2014;5:3935.
  111. Nishimura Y, Natsume A, Ito M, Hara M, Motomura K, Fukuyama R, et al. Interferon- $\beta$  delivery via human neural stem cell abates glial scar formation in spinal cord injury. *Cell Transplant*. 2013;22:2187–201.
  112. Chawla M, Kumar R, Siril PF. High catalytic activities of palladium nanowires synthesized using liquid crystal templating approach. *J Mol Catal A Chem*. 2016;423:126–34.
  113. Dutt S, Kumar R, Siril PF. Green synthesis of a palladium–polyaniline nanocomposite for green Suzuki–Miyaura coupling reactions. *RSC Adv*. 2015;5:33786–91.
  114. George J, Hsu CC, Nguyen LTB, Ye H, Cui Z. Neural tissue engineering with structured hydrogels in CNS models and therapies. *Biotechnol Adv*. 2020;42:107370.
  115. Tam RY, Fuehrmann T, Mitrousis N, Shoichet MS. Regenerative therapies for central nervous system diseases: a biomaterials approach. *Neuropsychopharmacology*. 2014;39:169–88.
  116. Skop NB, Calderon F, Cho CH, Gandhi CD, Levison SW. Optimizing a multifunctional microsphere scaffold to improve neural precursor cell transplantation for traumatic brain injury repair. *J Tissue Eng Regen Med*. 2016;10:E419–32.
  117. Omidinia-Anarkoli A, Boesveld S, Tuvshindorj U, Rose JC, Haraszi T, De Laporte L. An injectable hybrid hydrogel with oriented short fibers induces unidirectional growth of functional nerve cells. *Small*. 2017;13:1702207.
  118. Chedly J, Soares S, Montebault A, Von Boxberg Y, Veron-Ravaille M, Mouffle C, et al. Physical chitosan microhydrogels as scaffolds for spinal cord injury restoration and axon regeneration. *Biomaterials*. 2017;138:91–107.
  119. Tang-Schomer MD, White JD, Tien LW, Schmitt LI, Valentin TM, Graziano DJ, et al. Bioengineered functional brain-like cortical tissue. *Proc Natl Acad Sci U S A*. 2014;111:13811–6.

120. Lancaster MA, Corsini NS, Wolfinger S, Gustafson EH, Phillips AW, Burkard TR, et al. Guided self-organization and cortical plate formation in human brain organoids. *Nat Biotechnol*. 2017;35:659–66.
121. d'Amora M, Giordani S. The utility of zebrafish as a model for screening developmental neurotoxicity. *Front Neurosci*. 2018;12:976.
122. Park JS, Park K, Moon HT, Woo DG, Yang HN, Park KH. Electrical pulsed stimulation of surfaces homogeneously coated with gold nanoparticles to induce neurite outgrowth of PC12 cells. *Langmuir*. 2009;25:451–7.
123. Yi DK, Nanda SS, Kim K, Selvan ST. Recent progress in nanotechnology for stem cell differentiation, labeling, tracking and therapy. *J Mater Chem B*. 2017;5:9429–51.
124. Pinkernelle J, Keilhoff G. Growth factor choice is critical for successful functionalization of nanoparticles. *Front Neurosci*. 2015;9:305.
125. Convertino D, Luin S, Marchetti L, Coletti C. Peripheral neuron survival and outgrowth on graphene. *Front Neurosci*. 2018;12:1.
126. Hossain I, Tan C, Doughty PT, Dutta G, Murray TA, Siddiqui S, et al. A novel microbiosensor microarray for continuous ex vivo monitoring of gamma-aminobutyric acid in real-time. *Front Neurosci*. 2018;12:500.
127. Ou Y, Buchanan AM, Witt CE, Hashemi P. *Frontiers in electrochemical sensors for neurotransmitter detection: towards measuring neurotransmitters as chemical diagnostics for brain disorders*. *Anal Methods*. 2019;11:2738–55.
128. Qiu B, Bessler N, Figler K, Buchholz MB, Rios AC, Malda J, et al. Bioprinting neural systems to model central nervous system diseases. *Adv Funct Mater*. 2020;30:1910250.
129. Seong JM, Kim BC, Park JH, Kwon IK, Mantalaris A, Hwang YS. Stem cells in bone tissue engineering. *Biomed Mater*. 2010;5:062001.
130. Demirtaş TT, Irmak G, Gümtüşderelioğlu M. A bioprintable form of chitosan hydrogel for bone tissue engineering. *Biofabrication*. 2017;9:035003.
131. Gong T, Xie J, Liao J, Zhang T, Lin S, Lin Y. Nanomaterials and bone regeneration. *Bone Res*. 2015;3:15029.
132. Eivazzadeh-Keihan R, Chenab KK, Taheri-Ledari R, Mosafer J, Hashemi SM, Mokhtarzadeh A, et al. Recent advances in the application of mesoporous silica-based nanomaterials for bone tissue engineering. *Mater Sci Eng C Mater Biol Appl*. 2020;107:110267.
133. Yi H, Rehman FU, Zhao C, Liu B, He N. Recent advances in nano scaffolds for bone repair. *Bone Res*. 2016;4:16050.
134. Shalumon K, Lai GJ, Chen CH, Chen JP. Modulation of bone-specific tissue regeneration by incorporating bone morphogenetic protein and controlling the shell thickness of silk fibroin/chitosan/nanohydroxyapatite core-shell nanofibrous membranes. *ACS Appl Mater Interfaces*. 2015;7:21170–81.
135. Tang W, Lin D, Yu Y, Niu H, Guo H, Yuan Y, et al. Bioinspired trimodal macro/micro/nano-porous scaffolds loading rhBMP-2 for complete regeneration of critical size bone defect. *Acta Biomater*. 2016;32:309–23.
136. Nazir MA. Prevalence of periodontal disease. *Int J Health Sci*. 2017;11:72.
137. Baranova J, Büchner D, Götz W, Schulze M, Tobiasch E. Tooth formation: are the hardest tissues of human body hard to regenerate? *Int J Mol Sci*. 2020;21:4031.
138. Hakki SS, Bozkurt SB, Türkay E, Dard M, Purali N, Götz W. Recombinant amelogenin regulates the bioactivity of mouse cementoblasts in vitro. *Int J Oral Sci*. 2018;10:1–10.
139. Tonk CH, Witzler M, Schulze M, Tobiasch E. Mesenchymal stem cells. In: *Essential current concepts in stem cell biology*. Springer; 2020. p. 21–39.
140. Ottensmeyer PF, Witzler M, Schulze M, and Tobiasch E Small molecules enhance scaffold-based bone grafts via purinergic receptor signaling in stem cells. *Int J Mol Sci*. 2018;19:3601.
141. El Khaldi-Hansen B, El-Sayed F, Schipper D, Tobiasch E, Witzleben S, Schulze M. Functionalized 3D scaffolds for template-mediated biomineralization in bone regeneration. In: Rahman A, editor. *Frontiers in stem cell and regenerative medicine research*. Bentham Science; 2017. p. 130–78.
142. Kim BC, Bae H, Kwon IK, Lee EJ, Park JH, Khademhosseini A, et al. Osteoblastic/cementoblastic and neural differentiation of dental stem cells and their applications to tissue engineering and regenerative medicine. *Tissue Eng Part B Rev*. 2012;18:235–44.
143. Xi Y, Wang Y, Gao J, Xiao Y, Du J. Dual corona vesicles with intrinsic antibacterial and enhanced antibiotic delivery capabilities for effective treatment of biofilm-induced periodontitis. *ACS Nano*. 2019;13:13645–57.
144. Bao X, Zhao J, Sun J, Hu M, Yang X. Polydopamine nanoparticles as efficient scavengers for reactive oxygen species in periodontal disease. *ACS Nano*. 2018;12:8882–92.
145. Zhang L, Wang Y, Wang C, He M, Wan J, Wei Y, et al. Light-activable on-demand release of nano-antibiotic platforms for precise synergy of thermochemotherapy on periodontitis. *ACS Appl Mater Interfaces*. 2019;12:3354–62.
146. Zare EN, Lakouraj MM, Mohseni M. Biodegradable polypyrrole/dextrin conductive nanocomposite: synthesis, characterization, antioxidant and antibacterial activity. *Synth Met*. 2014;187:9–16.
147. Zhao X, Li P, Guo B, Ma PX. Antibacterial and conductive injectable hydrogels based on quaternized chitosan-graft-polyaniline/oxidized dextran for tissue engineering. *Acta Biomater*. 2015;26:236–48.
148. Tandon B, Magaz A, Balint R, Blaker JJ, Cartmell SH. Electroactive biomaterials: Vehicles for controlled delivery of therapeutic agents for drug delivery and tissue regeneration. *Adv Drug Deliv Rev*. 2018;129:148–68.

**Publisher's Note** Springer Nature remains neutral with regard to jurisdictional claims in published maps and institutional affiliations.